Molecular characteristics of ECSIT: Implications in Prostate Cancer

Thesis submitted for the degree of

DOCTOR OF PHILOSOPHY

To

THE DEPARTMENT OF ANIMAL BIOLOGY SCHOOL OF LIFE SCIENCES UNIVERSITY OF HYDERABAD HYDERABAD – 500046 INDIA



Nyshadham Sai Naga Chaitanya

Under the supervision of

Dr. A. Bindu Madhava Reddy

University of Hyderabad

Dept. of Animal Biology School of Life Sciences University of Hyderabad Hyderabad- 500 034

December 2022

Enrolment No: 16LAPH04

CERTIFICATE

This is to certify that this thesis entitled "Molecular Characteristics of ECSIT: Implications in Prostate Cancer." Submitted by Mr. Nyshadham Sai Naga Chaitanya bearing registration number 16LAPH04 in partial fulfilment of the requirements for the award of Doctor of Philosophy in the Department of Animal Biology, School of Life Sciences, is a bonafied work carried out by him under my supervision and guidance. This thesis is free from plagiarism and has not been submitted previously in full or parts have not been submitted to any other University or Institution for the award of any degree or diploma.

Parts of this thesis have been:

A. Presented in the following conferences

✓ All India Cell Biology conference, BITS Pilani GOA campus, GOA 21-23 DEC2018.

B. Published

- ✓ Chaitanya NSN, Tammineni P, Nagaraju GP, Reddy AB. Pleiotropic roles of evolutionarily conserved signaling intermediate in toll pathway (ECSIT) in pathophysiology. J Cell Physiol. 2022 Jul 19. doi: 10.1002/jcp.30832. Epub ahead of print. PMID: 35853181.
- ✓ Pandey M, Singh M, Wasnik K, Gupta S, Patra S, Gupta PS, Pareek D, Chaitanya NSN, Maity S, Reddy ABM, Tilak R, Paik P. Targeted and Enhanced Antimicrobial Inhibition of Mesoporous ZnO-Ag₂O/Ag, ZnO-CuO, and ZnO-SnO₂ Composite Nanoparticles. ACS Omega. 2021 Nov 16;6(47):31615-31631.

Further, the student has passed the following courses towards fulfilment of coursework

Course code	Course	Credits Resu	
AB 801	Analytical Techniques	4 Pas	
AB 802	Research ethics, Data analysis & Biostatistics	3	Pass
AB 803	Lab work & Seminar	5	Pass

Dr. A. Bindu Madhava Reddy

Assistant Professor
Dept. of Animal Biology
School of Life Sciences
University of Hyderabad
Hyderabad-500 046.

K. Sommeson

Head, Department of Animal Biology

अध्यक्ष / HEAD जंतु जैविकी विभाग Department of Animal Biology Monar Kundr Dean, Aly School of Life Sciences

School of Life Sciences University of Hyderabad Hyderabad 500 046.



University of Hyderabad

School of Life Sciences

Department of Animal Biology

Hyderabad-500 046, India

DECLARATION

I, Mr. N.S.N Chaitanya hereby declare that this thesis entitled "Molecular characteristics of ECSIT: Implications in Prostate Cancer" submitted by me under the guidance and supervision of Dr. A. Bindu Madhava Reddy, is an original and independent research work. I also declare that it has not been submitted to any other University or Institution for the award of any degree or diploma.

Date: 05-12-2022

N.S.N Chartanya

16LAPH04



University of Hyderabad School of Life Sciences Department of Animal Biology Hyderabad-500 046, India

CERTIFICATE

This is to certify that this thesis entitled "Molecular characteristics of ECSIT: Implications in Prostate Cancer" submitted by Mr. Nyshadham Sai Naga Chaitanya bearing registration number 16LAPH04 for the degree of Doctor of Philosophy to the University of Hyderabad is a Bonafede record of research work carried out by in the Department of Animal Biology, University of Hyderabad, Hyderabad under my supervision. The contents of this thesis, in full or parts have not been submitted to any other University or Institution for the award of any degree or diploma. I hereby, recommend her thesis for submission, for the award of the degree of Doctor of Philosophy from the University.

Madhava Reddy

Supervisor

Dr. A. Bindu Madhava Reddy Assistant Professor Dept. of Animal Biology School of Life Sciences University of Hyderabad Hyderabad-500 046.

Head,

K. Soummerson

Department of **Animal Biology**

अध्यक्ष / HEAD जंत् जैविकी विभाग Department of Animal Biology

Bus Kuch Dean, Aly School of Life

School Sciences University of Hyderahad Hydera: ... 500 046

Acknowledgement

- ❖ I acknowledge my supervisor **Dr. A. Bindu Madhava Reddy** for supporting me and providing me space to work in his lab.
- ❖ I acknowledge my doctoral committee members Dr. Nooruddin Khan and Prof. Kota Arun Kumar for providing me valuable suggestions during my research.
- ❖ I acknowledge Dean School of life science Prof. Siva Kumar, Prof. Dayanada Siddavattam and former deans Prof. K.V.A. Rammaiah, Prof. P. Reddanna for allowing me to utilise school facilities.
- ❖ I acknowledge Head of Department Animal Biology Prof. Sreenivasulu Kurukuti and former heads Prof. Anita Jagota, Prof. Jagan Mohan Rao for allowing me to utilise departmental facilities.
- ❖ I acknowledge my present and past Lab members Dr. S. Chenna kesavulu, Dr. C. Suresh, Mrs. Gayatri, Ms. Navya, Mr. Abhaya, Mrs. Charitha, Ms. Elina and project students Mr. Samir Bera, Ms. Priya maddhesiya, Mr. Mohd Saquib, Mr. Kartikey Saxena for their cooperation during my stay in the lab.
- ❖ I acknowledge Mr. Nandu Singh Thakur lab assistant for his support.
- ❖ I acknowledge Mrs. Leena Bhashyam and Dr. Praveen for FACS instrument, Mr. Prasad and Mr. Dasaradh for CD instrument, Dr. Prasad Tammineni for super resolution microscope, and Dr. Surya for bioinformatics.
- ❖ I acknowledge Dr. Insaf Ahmed Qureshi, Prof. Kota Arun Kumar, and Dr. Aruna Sree M.K and Dr. Jagan Mohan Reddy for allowing me to utilise their laboratory instruments.
- ❖ I acknowledge Dr. Vasudeva Rao, Dr. Narasaiah, Dr. Ram Gopal Reddy, and Dr. Phaniendra for their valuable suggestions in my research.
- ❖ I acknowledge funding body ICMR in providing me fellowship and DST, DBT, DAE funding for our lab.
- ❖ I am grateful to my parents for supporting me during my Ph. D.
- ❖ I thank almighty for blessing me.

Table of Contents

		Page no.
Review of literat	ure	1-12
1. Introduction		
2. Role of ECSI	Γ in cellular physiology	
2.1. Role of E0	CSIT in redox metabolism	
2.2. Role of E0	CSIT in innate immunity	
2.3 Role of EC	CIST in development	
3. Role of ECSIT	in pathological conditions	
3.1. ECSIT role in	n alzheimer's disease	
3.2. ECSIT role in	n viral infections	
3.3. Role of ECS1	T in hemochromatosis	
3.4 Role of ECS	T in cancer	
Rationale & obje	ectives	13
4. Mechanistic r	ole of ECSIT in prostate cancer cells	14-33
4.1 Demo	ography of prostate cancer	
4.2 Backs	ground	
4.2.1	Anatomy and histology of prostate gland	
4.2.2	Functions of prostate gland	
4.2.3	Genes associated with prostate cancer	
4.2.4	Diseases associated with prostate gland	
4.2.5	Types of prostate cancer	
4.2.6	Adenocarcinoma (prostate cancer)	
4.2.7	Signaling pathways in prostate cancer	
4.2.8	Risk factors and medication	
4.2.9	Detection, stages and treatment	
4.3 Metho	odology followed for objective I	
4.3.1	Cell lines used for the study and growth condition	
4.3.2	Plasmids used in this study	
4.3.3	Ribose nucleic acid (RNA) isolation	

4.3	6.4 Quai	ntitative real time Polymerase Chain Reaction	
4.3	3.5 Gene	eration of ECSIT knockdown cell line	
4.3	3.6 Cell	proliferation / Cell viability assay	
4.3	3.7 Fluo	rescence activated cell sorting (FACS)	
4.3	3.8 Trea	tment and cell cycle synchronization	
5.0 Results			
5.1 ECSIT ex	pression 1	evels were found to be high in prostate cancer	
5.2 Abrogatio	n of ECS	Treduces proliferation and survival of prostate cancer cel	lls
5.3 ECSIT Kı	ockdown	display delayed cell cycle progression	
5.4 The delay	in cell cy	cle was due to altered proliferative cell signalling	
5.5 Cell survi	val and ce	ell death pathways were altered under ECSIT knockdown	conditions
6.0 Characte	risation o	f ECSIT: In-silico and in-vitro approach	34-52
6.1 Int	roduction		
6.2 M	aterials us	ed and methodology followed for objective II	
6.	2.1 Cell li	nes used for the study and growth condition	
6.	2.2 Plasm	ids used in this study	
6.	2.3 Reage	ents used in this study	
6.	2.4 In-sili	co prediction of ECSIT mitochondrial localisation	
6.	2.5 Three	dimensional structure and molecular dynamics simulation	of ECSIT
6.	2.6 Molec	cular cloning (Traditional)	
6.	2.7 Polym	nerase chain reaction for cDNA amplification	
6.	2.8 Site d	irected mutagenesis	
6.	2.9 Agaro	se Gel Electrophoresis	
6.	2.10 Tran	sfection	
6.	2.11 Prote	ein Expression in prokaryotic host	
6.	2.12 Prote	ein Purification of His tag using Ni-NTA column	
6.	2.13 Imm	unoblotting	
6.	2.14 Oxid	ative stress	
6.	2.15 Circu	ılar dichroism (CD)	
6.	2.16 Fluo	rescence spectroscopy	
6.	2.17 Estir	nation of Reactive Oxygen Species using DCFDA	
6.	2.18 Imm	unofluorescence	
6.	2.19 Stati	stical analysis	

- 6.2.20 Oligonucleotides used in this work
- 6.2.21 List of Antibodies used in this work

7.0 Results

- 7.1 *In-silico* modeling of ECSIT structure
- 7.2 Molecular dynamics simulation of ECSIT with other protein shows preferential binding
- 7.3 *In-vitro* CD and Fluorescence spectroscopy data shows a structural change with Hydrogen Peroxide.
- 7.4 Import assay reveals wild type protein translocates to mitochondria compared to triple mutant (C14, 21,43A)

8. Conclusion	53
9. Discussion	54-56
10. Publications	57
11. References	58-63

Antiplagiarism certificate

List of Tables

- Table 1: Isoforms of ECSIT with varying exons and its amino acids with their mol. weight.
- Table 2: Effects of ECSIT upon interaction with respective proteins.
- Table 3: Summary of literature showing role of ECSIT under stress condition.
- Table 4: List of reagents used.
- Table 5: List of lentivirus sequences obtained from Dr. Gangisetty Subbarao Lab, Indian Institute of Science, India.
- Table 6: Primers used for real time PCR.
- Table 7: Primers used for cloning.
- Table 8: Antibodies used.

List of Figures

- Fig. 1: ECSIT structure and its interactions.
- Fig. 2: ECSIT in innate immunity.
- Fig. 3: ECSIT in BMP signaling.
- Fig. 4: ECSIT in RLR signaling.
- Fig. 5: ECSIT in Hepcidin regulation.
- Fig. 6: Cancer prevalence statistics around the world.
- Fig. 7: National cancer registry reports 2021.
- Fig. 8: Advancement of prostate cancer and their associated signaling pathways.
- Fig. 9: Molecular mechanisms for AR dependent pathways in castrate resistant prostate cancer cells.
- Fig. 10: Signaling pathways (androgen independent) in prostate cancer.
- Fig. 11: Prostate cancer stages and treatment.
- Fig. 12: ECSIT expression was found to be high in prostate cancer.
- Fig. 13: ECSIT knockdown shows less cell proliferation & survival rate.
- Fig. 14: ECSIT shows less proliferation rate due to either JAK/STAT or HIPPO/YAP signaling in DU145 cells.
- Fig. 15: Hampered Molecular Signaling Pathways under ECSIT knockdown.
- Fig. 16: Ablation of ECSIT attenuate tumorigenesis either by apoptosis or by autophagy in prostate cancer cells.
- Fig. 17: Privileged interaction on ECSIT determines its perspicuous role.
- Fig. 18: Prediction of Mitochondrial signal sequence through MitoprotII server.
- Fig. 19: Prediction of subcellular localisation through DeepMito webserver.

- Fig. 20: Procedure for site directed mutagenesis by overlap pcr method.
- Fig. 21: Modelling of ECSIT N-terminal and three-dimensional whole protein structure.
- Fig. 22: Molecular dynamic simulations of ECSIT.
- Fig. 23: In-vitro purified protein shows structural alteration under hydrogen peroxide treatment.
- Fig. 24: Protein (ECSIT) import into Mitochondria.

Abbreviations

AP-1 = Activator protein 1
AR = Androgen receptor

 $A\beta$ = Amyloid beta protein

BMP = Bone morphogenic protein

BPH = Benign prostatic hyperplasia

Ca+2 = Calcium ions

CARD = Caspase activation and recruitment domain

CD = Circular dichroism

cDNA = Complementary Deoxyribose nucleic acid

COX-2 = Cyclo-oxygenase 2

 CO_2 = Carbon dioxide

CRBN = Cereblon

CT = Computerised tomography

DAPI = 4',6-diamidino-2-phenylindole

DCFDA = Dichlorodihydro fluorescein Diacetate

DEPC = Diethylpyrocarbonate

DHT = Dihydrotestosterone

DMSO = Dimethylsulphoxide

DMEM = Dulbecco modified eagle medium

DNTP = Deoxy ribose nucleotide tri phosphate

ECSIT = Evolutionarily Conserved Signaling Intermediate in Toll pathway

EGFR = Epidermal growth factor receptor

ER = Endoplasmic reticulum

FACS = Fluorescence activated cell sorting

FBS = Fetal Bovine Serum

GAPDH = Glyceraldehyde phosphate dehydrogenase

 H_2O_2 = Hydrogen Peroxide

HBx = Hepatitis virus B x protein

HEK293T = Human embryonic kidney cells

HeLa = Henrietta Lacks

HFE = Human homeostatic iron regulator protein

HJV = Hemojuvelin

HRP = Horse radish peroxidase

IF = Immunofluorescence

IFN = Interferon

IKK = Inhibitor of nuclear factor-κB kinase

IL10 = Interleukin 10

IL-1R = Interleukin 1 receptor

IL-6 = Interleukin 6

IPTG = Isopropylthiogalactoside

IRAK = Interleukin-1 receptor associated kinase

IRF = Interferon Regulatory Factor

JAK = Janus kinase

K = Kelvin

LINCS = LINear Constraint Solver

LPS = Lipopolysaccharide

MD = Molecular Dynamics

MDA-5 = Melanoma differentiation-associated protein 5

MKK = Mitogen-activated protein kinase kinase

MRI = Magnetic resonance imaging

mRNA = Messenger ribose nucleic acid

mROS = Mitochondrial reactive oxygen species

MST = Mammalian STE20-like

MTS = Mitochondrial targeting sequence

MTT = 3-(4,5-dimethylthiazol-2-yl)-2,5-diphenyltetrazolium bromide

MyD88 = Myeloid differentiation primary response 88

NADPH = Reduced nicotinamide adenine dinucleotide phosphate

NaCl = Sodium chloride

 NaH_2PO_4 = Sodium dihydrogen phosphate

NVT = NVT ensemble

NDUFAF1 = NADH: Ubiquinone Oxidoreductase Complex Assembly Factor 1

NFkB = Nuclear Factor kappa-light-chain-enhancer of activated B cells

Ni-NTA = Nickel-Nitrilotriacetic acid

NLS = Nuclear localization sequence

NMDA = N-methyl-D-aspartate receptor

NO = Nitric oxide

NPT = NPTensemble

ns = nano second

OD = Optical density

p62 = Protein 62

PAMP = Pathogen-associated molecular patterns

PBS = Phosphate buffered saline

PCR = Polymerase chain reaction

PET = Positron emission tomography

PI = Propidium Iodide

PI3K = Phosphoinositide-3-kinase

PIC = Protease inhibitor cocktail

PKC α = Protein kinase C alpha

PKR = Protein kinase RNA-activated

PRDX = Peroxiredoxin

ps = pico second

PSA = Prostate specific antigen

PSEN = Presenlin

PTP = Protein tyrosine phosphorylation

QMEAN = Qualitative Model Energy ANalysis

Rac = Rho family of GTPase

RIG-1 = Retinoic acid-inducible gene I

RLR = Rig1 like receptor

ROS = Reactive oxygen species

SDS PAGE = Sodium dodecyl sulphate polyacrylamide gel electrophoresis

SMAD4 = Mothers against decapentaplegic homolog 4

SOCS = Suppressor of cytokine signaling

STAT = Signal transducer and activator of transcription

TAK-1 = TRAF associated kinase 1

TBK1 = TANK-binding kinase 1

TBST = Tris Base Saline Tween

TFR2 = Transferrin receptor 2

TGF- β = Tumor growth factor-beta

TIRAP = Toll/interleukin-1 receptor domain-containing adapter protein

TLR = Toll like receptor

TLx = T cell Leukaemia Homeobox

TMEM126B = Transmembrane Protein 126B

TNF α = Tumor necrosis factor alpha

TRAF = Tumor necrosis factor receptor—associated factor

TRAF3 = TNF Receptor Associated Factor 3

TRAF6 = Tumor necrosis receptor associated factor 6

TRIF = TIR-domain-containing adapter-inducing interferon-β

TRIM59 = Tripartite Motif Containing protein 59

UBE2N = Ubiquitin Conjugating Enzyme E 2N

UEV1A = Ubiquitin-conjugating enzyme E2 variant 1A

UV = Ultra violet

VISA = Virus-induced signaling adaptor

VSV = Vesicular stomatitis virus

YAP = Yes associated protein

⁰c = Degree Celsius

mM = Millimolar

rpm = Rotations per minute

nm = Nanometre

mg = Milligram

ul = Microliter

ng = Nanogram

ug = Microgram

Review of Literature

1. Introduction

ECSIT is an extremely conserved protein that is expressed in multiple tissues of invertebrates and higher chordates [1-5]. Though many putative isoforms are present, only two isoforms of ECSIT have been characterized. The number of exons and length of these isoforms differ. For instance, isoform 1 is the longest and consist of eight exons, while isoforms 2 and 3 are comprised of 7 and 5 exons, respectively. Interestingly, some putative isoforms incorporate only 2-3 exons. However, additional experimental studies are needed to test how the expression of these isoforms are regulated and their functional relevance during various pathophysiological conditions (Table 1). ECSIT predominantly located in the cytosol, but it can also be found in mitochondria and nucleus. [6]. It has an N-terminal mitochondrial targeting sequence (MTS) and a putative nuclear localization signal sequence (NLS). Other functional domains of ECSIT make a significant contribution to its involvement in various cellular processes Fig.1A. For example, ECSIT has a TRAF6 interacting domain (200-257) essential for its interaction with TRAF6 protein [7], while RIG1 and MDA5 bind at 268-431 during viral infection [8]. TRAF associated kinase 1(TAK1) binds to ECSIT at 300-431 amino acid region for Nuclear Factor kappa-light-chain-enhancer of activated B cells (NF-κB) activation [9], while allowing NF-κB release and translocation in to the nucleus, which eventually upregulates multiple target genes.

Interestingly, some of the functional domains of ECSIT have overlapping functions. For instance, Peroxiredoxin 6 interacts with ECSIT and its binding domain overlaps with TRAF6, suggesting the possibility for competitive binding [10]. Together, accumulating evidence indicates that ECSIT can participate in diverse physiological processes because of its distinct functional domains. However, additional studies are warranted to understand how protein-protein interactions regulate the phenotypic plasticity of ECSIT. Ubiquitination of ECSIT is a known posttranslational modification that is important for NF-κB stimulation in the cytosol and mitochondrial ROS production **Fig.1B.** The systematic study of how posttranslational modifications regulate its interaction could provide more information about how this protein functions in a specific cell organelle. The interaction of ECSIT with its respective binding partners and its effect on binding have been presented in **Table 2**.

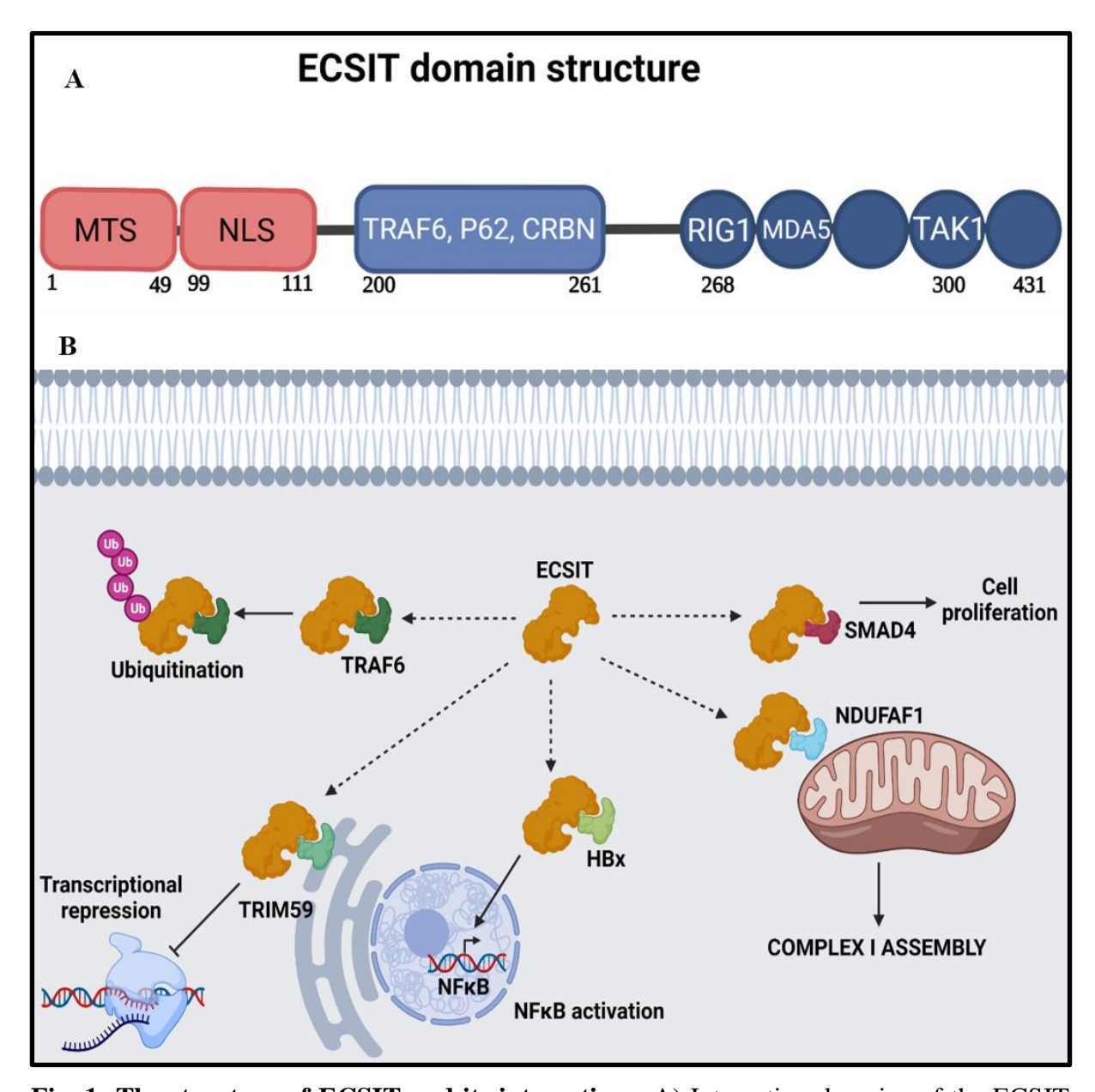


Fig. 1: The structure of ECSIT and its interactions. A) Interacting domains of the ECSIT with various proteins shown with specific amino acid residues. B) Effects of various proteins upon interaction with ECSIT.

Table 1: Isoforms of ECSIT with varying exons and its amino acids with their mol. weight.

Isoforms	No. of exons	Amino acids	Mol. weight
ECSIT 1	8	431	49KDa
ECSIT 2	7 (lacking 6)	296	33 KDa
ECSIT 3	5 (lacking 1, 2, 3)	217	24 KDa
ECSIT 4	4 (lacking 1, 6, 7, 8)	296	~34 KDa
ECSIT 5	2 (lacking 1, 4, 5, 6, 7, 8)	-	-
ECSIT 6	3 (lacking 4, 5, 6, 7, 8)	-	-
ECSIT 7	4 (lacking 2, 6, 7, 8)	-	-
ECSIT 8	3 (lacking 4, 5, 6, 7, 8)	-	-
ECSIT 9	2 (lacking 1, 4, 5, 6, 7, 8)	-	-
ECSIT 10	2 (lacking 1, 2, 5, 6, 7, 8)	-	-

Table 2: Effects of ECSIT upon interaction with respective proteins.

Interacting proteins of ECSIT	Effects
HBx (domain uncharacterised)	NF-κB activation
NDUFAF 1 (domain uncharacterised)	Complex I assembly
TRAF-6	Production of mROS in macrophage
SMAD 4 (domain uncharacterised)	Epiblast proliferation and mesoderm formation
RIG-1, MDA-5	IFNB1 production
P62	Inhibits NF-кВ activation & autophagy
CRBN	Inhibits bactericidal activity & autophagy
Pink1, Parkin, LC3B (domain uncharacterised)	Mitophagy

2. Role of ECSIT in cellular physiology

2.1. Role of ECSIT in redox metabolism

ROS produced within the cell as a result of aerobic metabolism. These highly reactive superoxide radicals, hydroxyl radicals, singlet oxygen and hydrogen peroxide species contribute to oxidative stress [11, 12]. Cells rely on intracellular antioxidant enzymes to protect themselves from ROS-induced oxidative damage. Any imbalance in the generation and clearance of free radicals results in ROS accumulation within the cell, which contributes to oxidative stress. In addition, mitochondria play an essential role in ROS metabolism. Intracellular pathogens and other signaling pathways target mitochondrial redox surveillance

systems to regulate redox homeostasis [13]. ECSIT is localized to mitochondria and controls mitochondrial ROS (mROS) by regulating complex I activity and mitochondrial quality control through its interaction with chaperone NADH: Ubiquinone Oxidoreductase Complex Assembly Factor 1 (NDUFAF-1) and transmembrane Protein 126B (TMEM126B) [14, 15]. ECSIT knockdown consistently results in impaired complex-I assembly as well as mitochondrial dysfunction [16]. In addition, loss of ECSIT prompts mitochondrial membrane depolarization and diminished parkin recruitment, resulting in the accumulation of dysfunctional mitochondria and increased mitochondrial ROS [17], which is imperative for bactericidal action of macrophage. Peroxiredoxin (PRDX) are critical antioxidant enzymes that are involved in redox homeostasis [18]. They regulate intracellular ROS through various signaling mechanisms [19]. Peroxiredoxin 6, the only mammalian Cys-prdx member, is involved in protection against oxidative stress[20]. It negatively regulates mitochondrial ROS production by disrupting the complex formation between TRAF6 and ECSIT. Together, these observations indicate that ECSIT regulates mROS production. Since the TRAF6-ECSIT complex is required for mROS production, and loss of interaction with TRAF6 reduces mROS production, ECSIT mediated ROS regulation could be guided by its interacting partners.

2.2. Role of ECSIT in innate immunity

Innate immune cells eliminate the invading bacteria through phagocytosis and this result in massive upregulation of reactive oxygen species (ROS). Besides mitochondrial OXPHOS, ROS production also occurs through NADPH oxidase [21, 22]. Toll-like receptors (TLR) play a vital role in innate immunity during bacterial and viral infections. Upon activation of the TLR pathway, TRAF-6 translocates to mitochondria [23] and enhances the host's susceptibility to intracellular infections [24]. TRAF6 mediated ubiquitination of ECSIT primarily results in increased mitochondrial ROS generation, which contributes to bactericidal action during TLR cascade. PRDX1 inhibits TLR signalling, resulting in decreased bacterial clearance. Studies have demonstrated that PRDX1 interaction with TRAF6 leads to TRAF6 mediated ubiquitination of ECSIT, which is critical in the activation of NF-κB in response to TLR-4 stimulation [25]. Immune functions of ECSIT are conserved across the species, as it is vital in offering protection against bacterial, virus, and fungal infections in the lower chordate suggesting the importance of ECSIT in immune mechanisms [1, 2, 26, 27]). Recent studies on crustaceans unveiled its anti-bacterial role along with TRAF6, which was inhibited through miRNA224 [28] Fig. 2a. Densely packed miRNA224 in exosomes leads to HSP70 suppression

and HSP70-TRAF6 disruption. Furthermore, the release of TRAF6 interacts with ECSIT to modulate mROS production. Additionally, this interaction regulates anti-lipopolysaccharide factor (ALFs) expression within the recipient's blood cell, ultimately attacking the homeostasis of the haemolymph microbiota due to infection in mud crab. In the course of an infection or tissue damage, injured cells secrete cytokines that signal lymphocytes to the site of the injury, resulting in inflammation. Several receptors (innate immunity), such as TLR and RIG1 like receptors (RLR) internal DNA sensors cGAS were employed to neutralize the pathogens [29, 30]. TLR signaling operates through myeloid differentiation 88 (MyD88) [31] or TRIF-β protein [32]. ECSIT is one of the downstream signaling proteins of the TLR pathway that modulates the activation of NF-κB transcription factor through MEKK-I [33]. TRAF-6 ubiquitinates ECSIT at the K372 position and translocated to the nucleus with activated p65 and p50 [7]. Inflammation can be controlled by altered NF-kB expression through Tripartite Motif Containing protein 59 (TRIM59) [34], protein 62 (P62) [35, 36], and cereblon (CRBN) [37] by an inhibitory mechanism Fig. 2b. Activation of NF-kB is a major event in the innate immune response. ECSIT regulates inflammation by activating NF-κB and protect cells from infections. One of the analogous mechanisms generated by LPS activates TLR4 signaling within cell routing through ECSIT thereby producing pro inflammatory cytokine mediating NFκΒ. Moreover, ECSIT is involved in innate immunity for regulation of bacterial infections. ECSIT is a downstream signaling target for myosin phosphatase target 1 subunit (MYPT1), which is essential for maintaining the contraction and healthy vasculature of VSMCs, thus regulating the blood brain barrier function [38]. MYPT1 deregulates ECSIT-IL6 axis and augments ischemic stroke, while loss of MYPT1 leads to disturbed blood brain barrier by enhanced expression of ECSIT-IL6.

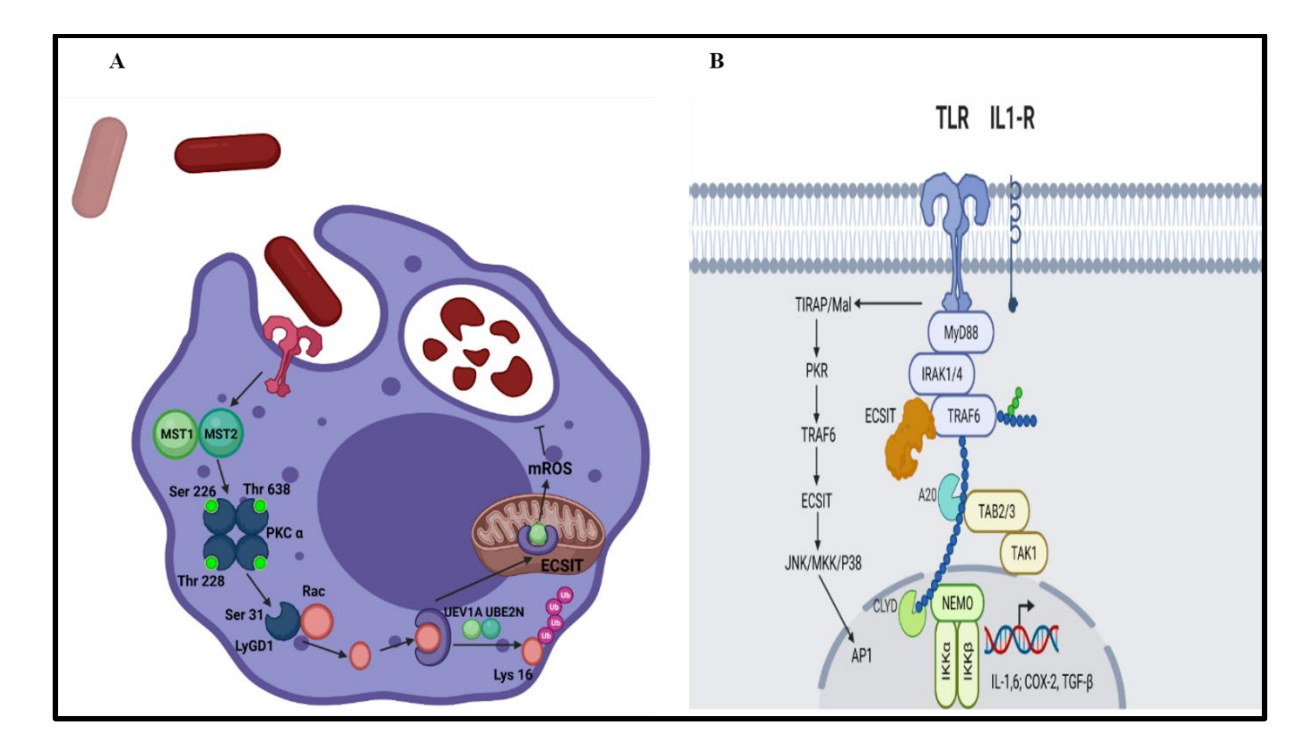


Fig. 2: ECSIT in innate immunity. (a) ECSIT in antibacterial immunity. Phagocytosed bacteria are destructed by mROS, which is produced from mitochondria through the interaction of ECSIT and TRAF-6 which is provided by the dissociation of activated Rac (produced through series of events) from TRAF-6 MATH domain. (b) ECSIT in TLR signaling. TLR4 signaling operates when stimulated by lipopolysaccharide (LPS) signaling cascade that occurs either by MyD88 dependent pathway or independently by activating NF-κB and AP-1.

2.3 Role of ECSIT in development

BMP (Bone morphogenetic protein) is a member of the transforming growth factor-β family and was first thought to induce bone formation from mesenchymal stromal cells. Later, it was shown that BMP signaling regulates apoptosis, cell growth, and differentiation [39-41]. BMP acts both through canonical and non-canonical pathways. BMP binds through extracellular Type I and II receptors in the canonical pathway and operates through Mothers against decapentaplegic homolog 4 (SMAD) proteins [42]. In the non-canonical pathway, BMP activates other signaling proteins, such as p38, cdc42, and TAK. Interestingly, a targeted null mutation of ECSIT resembles the phenotypic plasticity of Bmp receptor type 1a null mutant suggesting the role of ECSIT in BMP signaling. Further, ECSIT interacts with both Smad1 and Smad4 to regulate the expression of explicit BMP target genes. Besides altered BMP and Toll signaling, ECSIT knockdown altered epiblast designing, reduced cell proliferation and

impaired mesoderm formation [43] Fig. 3. Further exploration is warranted to understand ECSIT's functional role in Smad pathways.

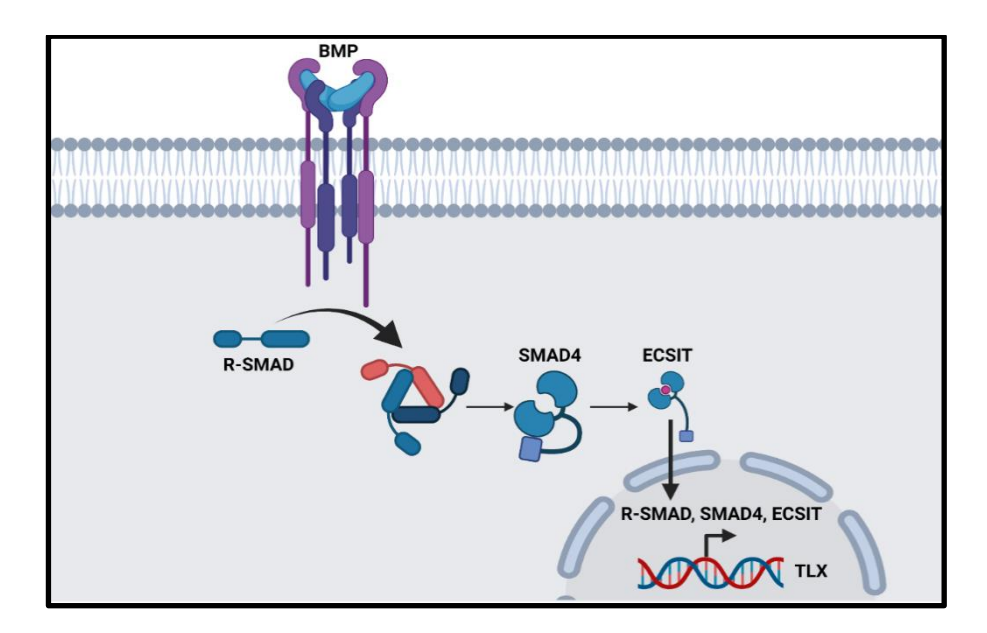


Fig. 3: ECSIT in BMP signaling. ECSIT gets activated with BMP receptor and regulates transcription of developmental genes with the help of SMAD protein intermediates in canonical pathway.

3. Role of ECSIT in pathological conditions

3.1. ECSIT role in Alzheimer's disease

Alzheimer's disease (AD) is identified by extracellular Amyloid-B plaques accumulation as well as intracellular hyper phosphorylated tau neurofibrillary tangles (NFTs). AD occurs in two forms early-onset Familial AD (FAD), which is purely genetic and late-onset Sporadic AD (SAD), which is caused due to both genetic and environmental factors [44-46]. A variety of pathways was found to be linked with the early onset or progression of AD; however, the etiology of AD remains unpredictable. According to recent studies the location of ESCIT gene in chromosome 19 (p13.2) is linked with increased AD risk [47]. Subsequently, bioinformatics studies revealed the interaction of ECSIT with various signaling pathways to be linked with AD. These observations in addition to several other investigations have led to the development of a model involving ECSIT that target AD. There is solid evidence that suggests the potential role of ESCIT in regulating inflammatory pathways as well as cell signaling responses towards injury through TLR and NF-κB pathways associated with AD pathogenesis. Further investigations are needed to test the predictions that ECSIT influences oxidative stress and

mitochondrial welfare. Moreover, ECSIT activity within various neural stem cells, neuroglia, and neurons is unexplored. Furthermore, it was shown that ECSIT has been identified as a fundamental node in the AD protein interaction networks (AD-PIN) with many interactions. It was hypothesized that ECSIT could integrate mitochondrial dysfunction, amyloid-B metabolism, and oxidative stress in AD pathogenesis based on its interaction with proteins such as PSEN1 and other redox as well as mitochondrial proteins that are encoded by ADsusceptibility genes [48]. ECSIT is primarily expressed in the cortex, hippocampus, and amygdala neurons. ECSIT is also found in different brain cells. ECSIT deletion in a subgroup of neurons results in the advancement of advanced neuropathology and this includes neuroinflammation, abnormal cognitive behaviour, tau pathology neuronal loss, and gliosis that are common symptoms of AD. ECSIT loss in the areas of brain affected by AD, leads to impaired mitophagy, complex I alterations, and mROS accumulation. Scavenging mROS with mitochondrial targeted human catalase (MCAT) delayed neuropathology in mice with decreased ECSIT expression, implying that mROS resulted from dysfunctional mitochondria is a major etiological factor in AD [49]. These findings suggest that ECSIT might play a role in mitochondrial quality control and maintenance, a failure of which could result in the neuropathologies discussed above, leading to the progression of AD.

3.2. ECSIT role in viral infections

ECSIT is transitional in TLR signaling, which is required for NF-κB stimulation and inflammation. It also plays a vital role in anti-viral response through the production of IFNB1 by interacting with CARD of RLR and transmembrane domain of virus-induced signaling adaptor (VISA) [8]. This further leads to the stimulation of Interferon Regulatory Factor (IRF-3) and interferon (IFN) genes. On the contrary, ECSIT knockdown results in abrogation of anti-viral response. Virally activated RIG-1 and melanoma differentiation-associated protein 5 (MDA-5) binds to ECSIT at 268-431 amino acid residue as well as promotes nuclear translocation of TNF Receptor Associated Factor 3 (TRAF-3) and IRF-3 Domain-mapping analysis using Cyto trap two-hybrid assay suggesting that ECSIT mediated NF-κB activation occurs through its interaction with hepatitis B virus X protein (HBX) [49]. It had been established that ECSIT regulates the production of interferons during viral infections Fig. 4.

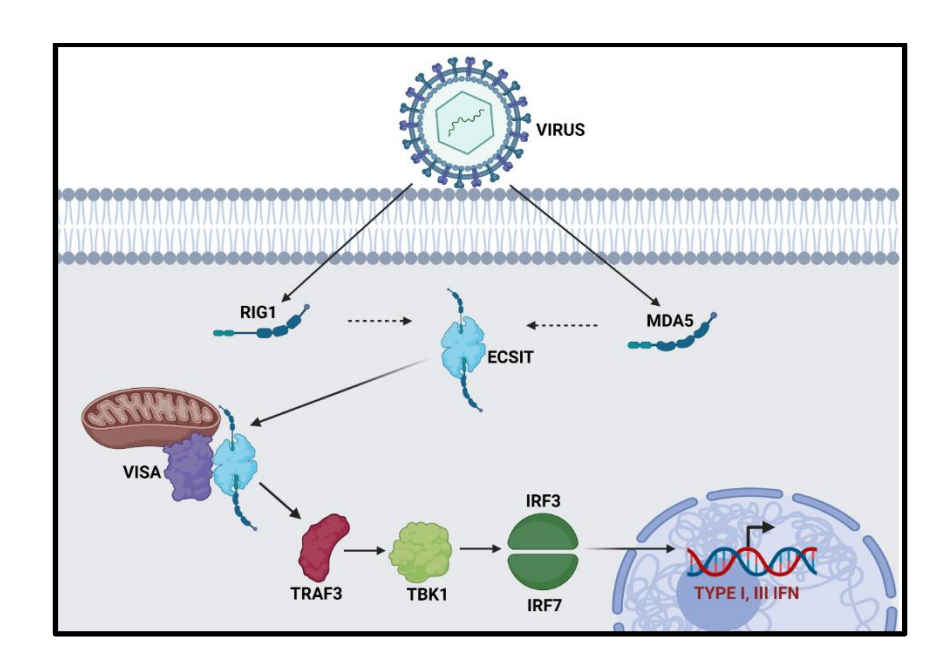


Fig. 4: ECSIT in RLR signaling. Viral infection activates RIG-1 and MDA-5 thereby interacting with ECSIT and translocates to mitochondria periphery to interact with VISA protein and help in transcription of interferon related genes.

3.3. Role of ECSIT in hemochromatosis

Hepcidin is an anti-microbial peptide that is produced in hepatocytes and regulates iron homeostasis. Its expression is upregulated in acute inflammatory responses or elevated iron levels. Overexpression of hepcidin leads to iron deficiency, while reduced expression contributes to an increased iron content in the body also known as hemochromatosis (Give references). The iron sensing and inflammatory pathways controls the hepcidin expression [50]. Inflammatory pathways regulate Hepcidin expression by the paracrine effect through kupffer cells or TLR-4 expression in peripheral myeloid cells [51]. Macrophages in the inflammatory pathway help synthesize the hepcidin expression through the production of interleukin 6 (IL6). This IL6 acts in paracrine fashion for kupffer cells in producing hepcidin protein. The iron sensing pathways involving non-immune cells such as hepatocytes regulate hepcidin through ECSIT and SMAD4 interaction. Hepcidin expression in hepatocytes also occurs by IL6 stimulation and downstream cascades involving signal transducer and activator of transcription (STATs) Fig. 5. Overall, ECSIT aids in the reduction of increased iron content in the body.

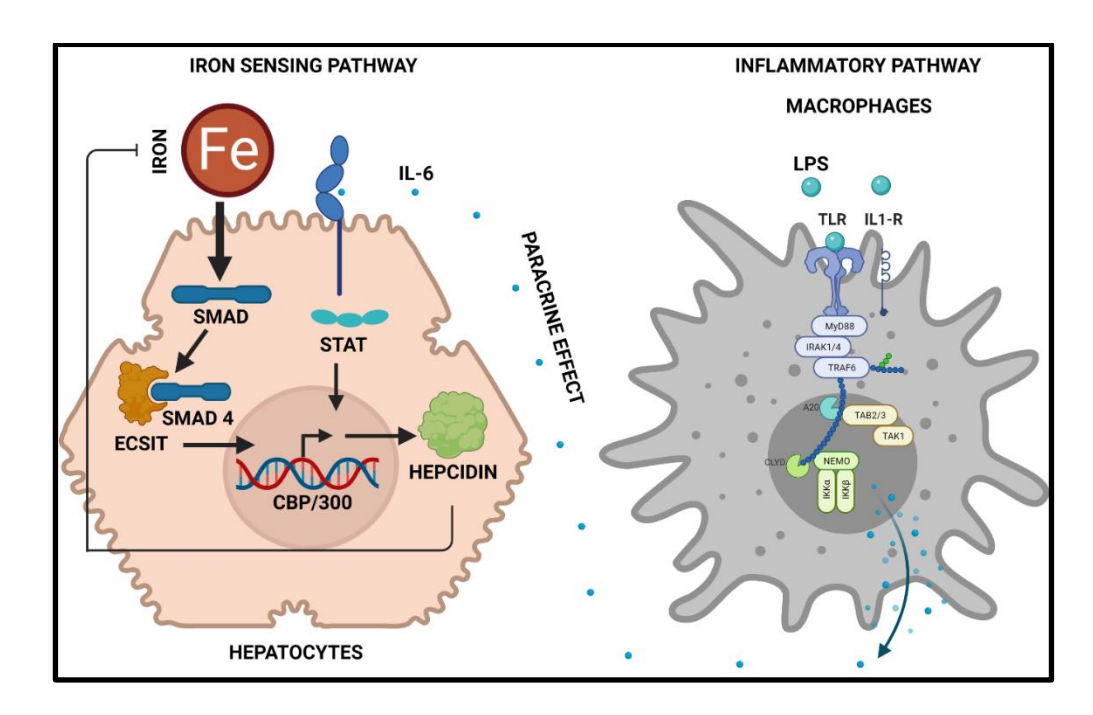


Fig. 5: ECSIT in Hepcidin regulation. Hepcidin protein produced in hepatocytes through iron sensing pathways, which sensed by iron overload and IL-6 produced from neighbouring cells upon infection with bacteria.

3.4 Role of ECSIT in cancer

Growing evidence suggests that ECSIT regulates tumorigenesis. For instance, ECSIT was shown to inhibit cell death by reducing the activation of caspase 3 in breast cancer cells as well as promote tumor progression through NFkB-p53 axis [52]. Whereas in leukaemia, proteomic screening reveals that ECSIT is one of the effectors of BCR-FGFR1 fusion proteins induced haematopoiesis observed in leukemic conditions [53]. These reports suggest that ECSIT exhibits a potential role in cancer metabolism. However, further studies are warranted to establish the precise function of ECSIT carcinogenesis. The summary of literature shown in Table 3.

Table 3: Summary of literature showing role of ECSIT under stress condition.

S.No	YEAR	PMID	Stress	Model system	Pathway	Genes upregulated	Ecsit localisation
1.	1999	10465784	LPS	HEK 293, Drosophila	TLR, TNF-α		Not determined
2.	2007	17187402	LPS		TLR4, JAK- STAT	IL-6, hepcidin	Cyto
3.	2007	17344420	Not determined	,	Not determined	Not determined	Cyto & Mito
4.	2011	21525932	LPS, Salmonella typhimuriu m	RAW 264.7, J774A.1, and NOR10	TLR4	Not determined	Mito
5.	2012	22588174	POLY(I:C)	Hela, HEK 293	TLR	IFNB, NFKB, IRSE	Mito
6.	2012	22389973	LPS	Dental pulp cells	TLR4,TGF-B	IL-6, TGF-B	Not determined
7.	2014	24796866	Vibrio anguillarum / Staphylococ cus aureus	Marsupenaeus japonicus	TLR	Anti-LPS factors 5,6	Not determined
8.	2015	26204814	V.alginolytic us, S.haemolytic us, S.Cerevisiae	Crassostrea Hongkongensis, HEK 293	TLR	Not determined	Cyto
9.	2015	25449573	IL-1B	Huh 7, HEK 293	NFkB	IL-10	Not determined
10.	2015	25355951	LPS	HEK 293, MEF	TLR 4	NFKB, IL 6, IL 1B, IRF 7	Cyto
11.	2016	28251965	Not determined	Amphioxus	TLR/BMP	Not determined	Not determined
12.	2017	28393051	LPS	HEK293T, THP-1	TLR4	Not determined	Cyto
13.	2018	29288875	TNF-α, POLY(I:C), LPS, noggin	СТРС	TLR, BMP	Smad1/5/8, IRF-3, MSX-2	Not determined
14.	2018	29929436	LPS	HEK293T, MDA MB231, THP-1, SK-HEP-1	· · · · · · · · · · · · · · · · · · ·	NFKB, IL 6, IL-1B, IER 3, CCL 5, BCL 2, LTA	Cyto
15.	2018	29514094	LPS	BMDM	Not determined	Not determined	Mito
16.	2019	31281713	LPS	HEK293T, THP-1, MEF	TLR-4	NFKB, IL 6, IL-1B, TNF-0	Cyto
17.	2019	31620128	LPS	HEK293T, THP-1, MEF	TLR-4	CRBN	Mito

Rationale & Objectives

Rationale of the study:

By participating in various signaling pathways, ECSIT activates various transcription factors responsible for cell proliferation and outcome of these cellular physiological processes were much related to cancer phenotype moreover partner-binding proteins were upregulated in various cancers we suspect its new possible role in cancer progression. To address this, we dissected the work into two parts first by studying its mechanistic role and then to characterise it.

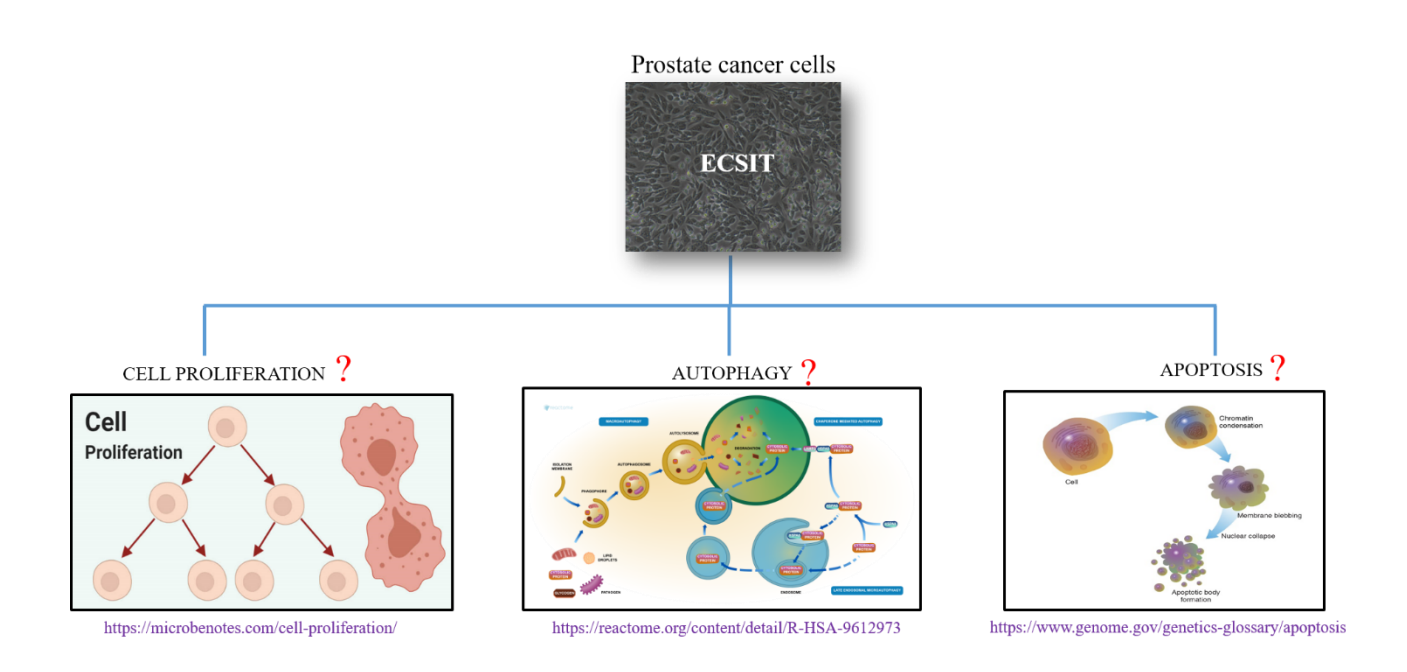
Objective I:

- ✓ Mechanistic role of ECSIT in prostate cancer cells.
 - Elucidation of ECSIT role in the context of cell proliferation.
 - Illustration of ECSIT's role as a new paradigm shift in autophagy.
 - Role of ECSIT in apoptosis.

Objective II:

- ✓ Characterisation of ECSIT: *in-silico* and *in-vitro* approach.
 - To document the structural change of ECSIT with its partner binding through molecular dynamic simulations.
 - To validate the *in-silico* work through Circular Dichroism, Fluorescence spectroscopy, and import assay.

Objective I: Mechanistic role of ECSIT in prostate cancer cells



4.1 Demography of Prostate Cancer

As per the world health organization (WHO), there will be approximately 1.1 million prostate cancer incident cases worldwide in 2020, the third highest among various cancers. The incidence had been found to be high in Australia, North America, Northern Europe, etc... and low incidence was observed in Asia and North Africa. Recently statistics data suggest cases were surging in Asian countries such as Japan, Singapore, etc...[54], according to globocan 2020 reports cancer is the leading cause of death in Asian countries, prostate cancer ranks second among various cancers in men all over the world. The summary of incidence and mortality of prostate cancer among men across various countries and with other cancer types were depicted in Fig. 6. According to the National Cancer Registry's (ICMR) 2021 report on prostate cancer, 80% of cases are reported in people National cancer registry (ICMR) 2021 report about prostate cancer declares that 80% of cases reported in people over 60 years, and according to the histological classification, says that adenocarcinoma makes up about 77% compared with other types, Systemic therapy was employed to treat the 42.9% of diseased patients who had been found to have distinct metastasis. Within 8-30days patients sought to found treatment at reporting hospital. The summary of the report is shown in Fig. 7. In India, the incidence of prostate cancer is expected to rise in the coming years as compared to previous years and population-based cancer registries state that Ahmedabad, Kollam, Kolkata, Kamrup, Mumbai, Delhi, Bangalore, Barshi, Bhopal, Chennai, Nagpur, Trivandrum were top cities according to incidence rates and less in Gujrat and Madhya Pradesh [55]. The proportional increase in the incidence of prostate cancer in India could be attributed to migration from rural to urban regions, changes in lifestyles, etc... [56]. Prostate cancer caused due to various factors such as age, ethnicity, environmental factors, and diet consumption, people who migrate from India to America had more chances to be prone. Therefore, there should be efficient prevention strategies by understanding the molecular mechanisms within it and preventing further spread, either by the usage of proper medication, following proper physical activity, use of advanced medical technology [57, 58].

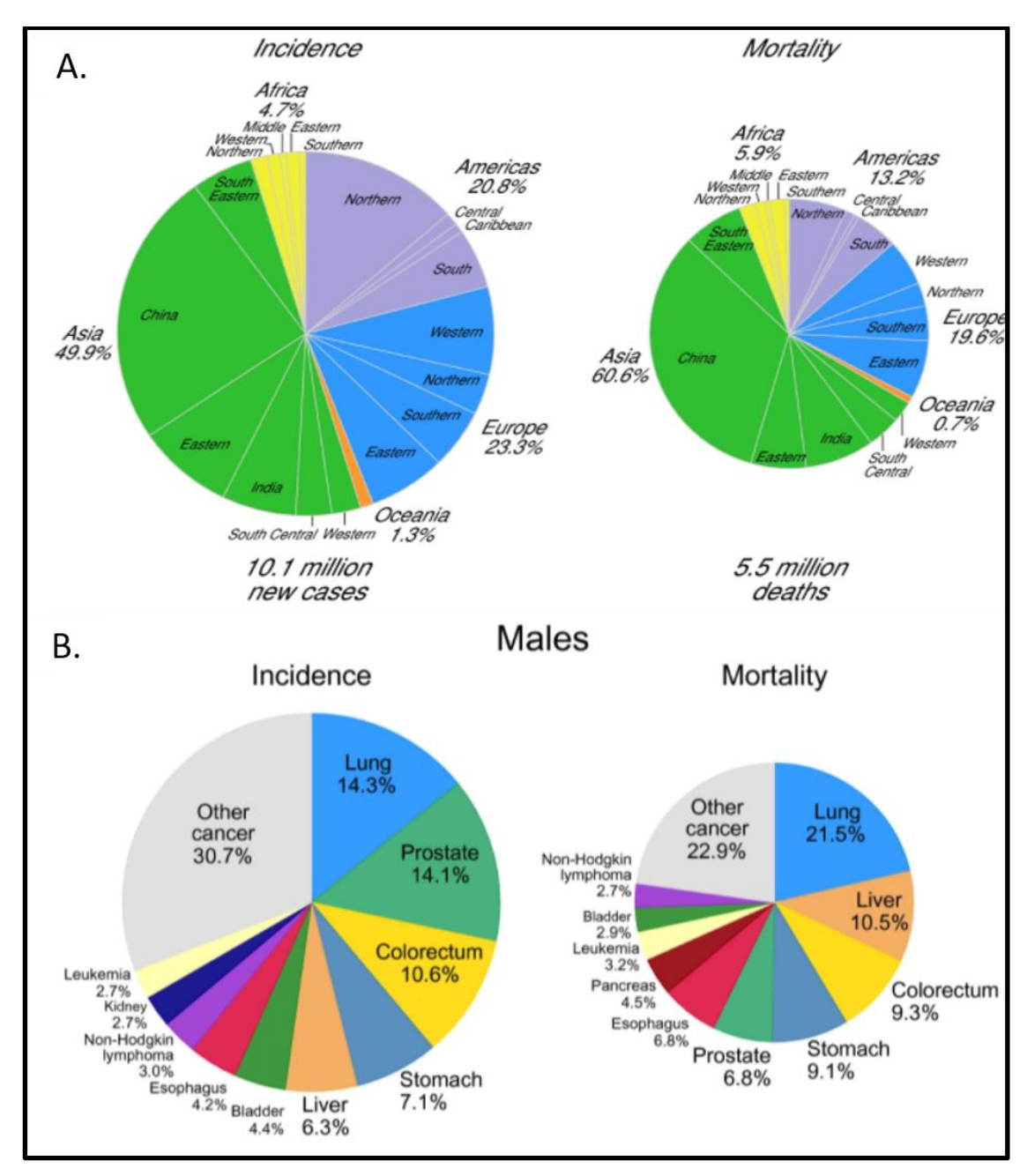


Fig. 6: Cancer prevalence statistics around the world (Adapted from globocon). A. Globocan 2020 cancer statistics among men in the world say cancer incidence and mortality were high in Asian countries. B. Globocan 2020 statistics for men among various cancers indicate other high follow incidences and mortality due to lung cancer.

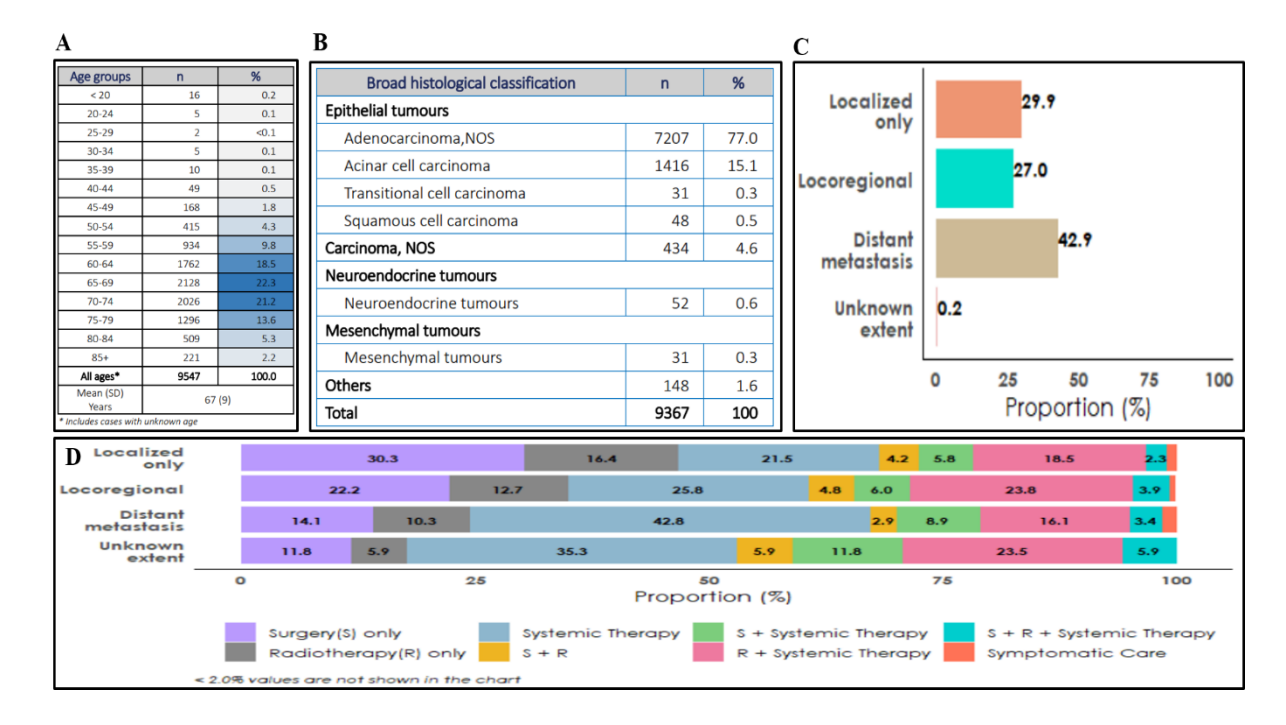


Fig. 7: National cancer registry reports 2021 (Adapted from ICMR). A. Five-year age group distribution of prostate cancer. B. Histological classification of number and proportion of prostate cancer. C. Clinical extent of prostate cancer among patients. D. Treatment type based on the extent of prostate cancer.

4.2 Background

4.2.1 Anatomy and histology of prostate gland

The prostate gland (part of the male reproductive system) produces fluid of semen located in the pelvic region and its size varies with age. Anatomically it is revealed that the prostate gland contains four zones Fibromuscular stroma (made of muscle and fibre), Central (surrounds ejaculatory duct), Peripheral (most cancers arise), Periurethral transition zone (surrounds urethra), histologically it has epithelial and stromal regions separated by basement membranes [59] Fig. 8. Epithelium (peripheral zone) had three distinct cells luminal, basal, and neuroendocrine cells on the basement membrane [60]. Malignant cells arise mostly from luminal cells; benign carcinoma originates from basal cells, and DU145 cells are derived from neuroendocrine cells.

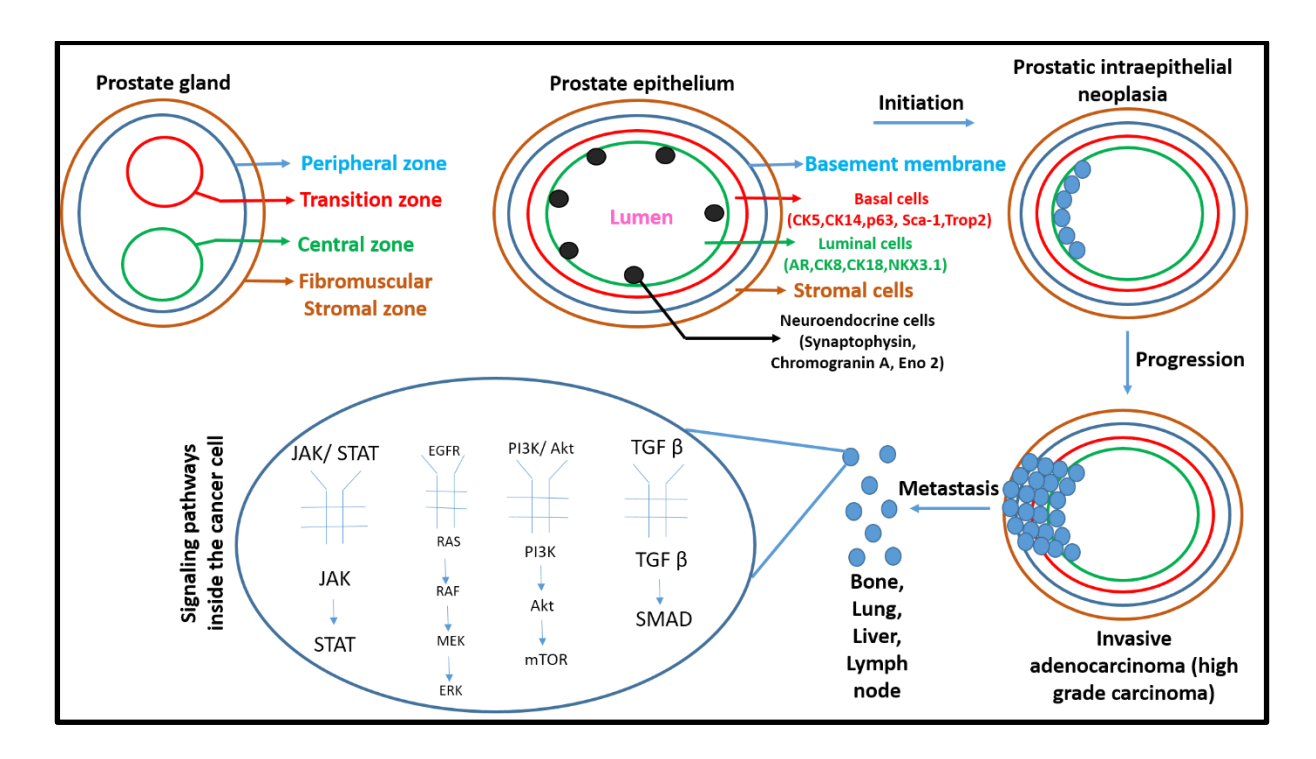


Fig. 8: Advancement of prostate cancer and their associated signaling pathways. The prostate gland had four zones fibromuscular layer, peripheral zone, periurethral transition zone, and central zone. The prostate epithelium has three layers of luminal cells (AR, CK8, CK18, NKX3.1) basal cells (CK5, CK14, p63, Sca-1, Trop2), and basement membrane surrounded by stromal cells. In between luminal, cells, there are neuroendocrine cells (Synaptophysin, Chromogranin A, and Eno2). Layer markers are represented in parentheses. There are three stages in prostate cancer development, which include initiation (either due to external or internal factors that forms intraepithelial neoplasia), Progression (cells replicate and form invasive carcinoma), which then migrates to other organs such as bone, lung, and liver and lymph node known as metastasis. Signaling pathways such as JAK/STAT, EGFR, PI3K/Akt, and $TGF\beta$ operate inside the cancerous cell for proliferation and migration to other tissues.

4.2.2 Functions of prostate gland

The prostate gland was used for fertility; the functions of the prostate gland include the production of prostatic fluid to semen. The prostatic fluid contains enzymes (prostate-specific antigen), Zinc, and citric acid. Apart from the production of semen, it also closes the urethra during ejaculation and converts testosterone into dihydrotestosterone (DHT) through 5-alpha reductase.

4.2.3 Genes associated with prostate cancer

The sustained proliferation of cells in the prostate gland and gradual loss of PTEN, lack of prostate-specific antigen (PSA) metastasizing to other organs leading to the formation of the tumor make a prostate cancer cell different from a normal cell. Prostate cancer was caused mainly due to mutations in DNA, genes of heredity involve BRCA 1,2; CHEK 2, ATM, PALB 2, RAD51D, MSH 2, MSH 6, MLH 1, PMS 2, RNASEL, HOXB 13 [61, 62]. Acquired cancer may be due to hormonal influences such as testosterone, insulin-like growth factor, radiation, and chemicals causing DNA damage [58]. Genetic changes in luminal cells of the prostate gland form lesions and spread to other tissue.

4.2.4 Diseases associated with prostate gland

Prostate cancer is the most common form in males next to skin cancer. People above the age of 60 were diagnosed with prostate cancer. The morphological changes of the prostate gland are a sign of diseased prostate. The morphological change may be due to an enlarged gland, inflamed gland, or formation of new tissue in the prostate gland. Men below the age of 50 suffered from prostatitis where swelling or inflammation of the prostate gland occurs. Prostatitis may be acute due to bacterial infections or chronic lasts for more than 3 months and cause pelvic pain. Males over 50 years of age suffered from enlarged prostate known as **benign** prostatic hyperplasia (BPH) (non-cancerous enlargement). The enlarged prostate compresses the urethra thereby preventing urine outflow and leading to the retention of fluid in the urinary bladder that becomes a problem and requires medical treatment. The formation of lesions in the gland due to either extrinsic or intrinsic factors or metastasizing to other tissue leads to a diseased phenotype known as prostate cancer. Although there were several transcriptional factors that were in common with BPH and prostate cancer, androgen signaling is driving prostate cancer while there were several factors responsible for BPH. BPH was not considered an initial step in the progression of prostate cancer. BPH is not malignant while prostate cancer is malignant, several common genetic functionalities shared for both include SRDAR2, CYP 17, CYP 19, 14-3-3α, RASSF1A **[63]**.

4.2.5 Types of prostate cancer

There are several different types of prostate cancers among which the most common is **adenocarcinoma**; others include small cell carcinoma, neuroendocrine carcinoma, transitional carcinoma, sarcoma, etc. Prostate cancer may be androgen-dependent or

independent based on the androgen receptor mechanisms. The deprivation of androgen therapy in androgen-dependent cancer could be a potential target for prostate cancer and makes androgen-dependent to castration-resistant cancer. Castration-resistant prostate cancer (CRPC) cells lead to the reactivation of androgen receptors and the presence of AR-negative cells. As an AR-dependent mechanism could be major, AR negative cell population could provide an additional mechanism for the progression of cancer and it had been identified that JAK2/STAT5 pathway may be one of the mechanisms targeting both pathways that leads to cell CRPC progression and survival [64]. Prostate cancer mostly arises in an androgen-dependent way Fig. 9 but deprivation of androgen causes cancer to progress as an androgen-independent mechanism. Targeting androgen-independent mechanisms was difficult and mechanisms that enhance AR-dependent signaling in CRPC include AR gene amplification, AR gene mutations, altered AR coregulatory proteins, aberrant androgen-generating pathways, ligand-independent activation of AR could provide efficient therapeutic strategies [65].

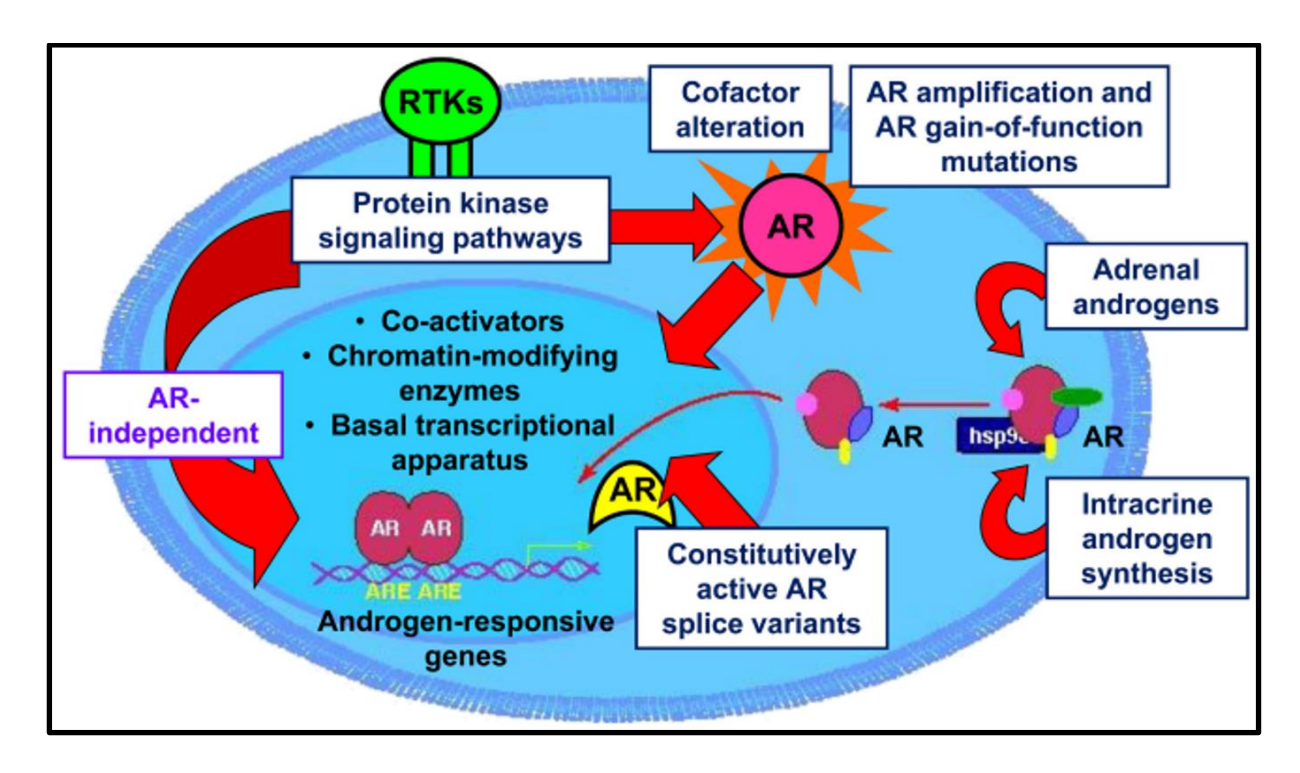


Fig. 9: Molecular mechanisms for AR-dependent pathways in castrate-resistant prostate cancer cells (Adapted from [64]). AR-dependent pathways are activated due to AR gene amplification, intra-androgen biosynthesis, AR splice variants, alteration of the cofactor of AR proteins, AR independent protein kinase pathways that lead to the activation of androgen-responsive genes.

4.2.6 Adenocarcinoma (prostate cancer)

Prostate cancer originates as inflammatory atrophy that converts localized to metastatic either through carcinogens or by cytokine-cytokine receptor interactions [63]. Prostate cancer progression occurs through three stages initiation, progression, and advancement. Prostate carcinoma is a multistep phenomenon where lesions develop in luminal epithelial cells to form new cells (Prostatic intraepithelial neoplasia (PIL)), PIL of the high grade was genetically similar to prostate carcinoma such as overexpression of BCL2, GSTP1, ki-67 and under expression of p27, PTEN, NKX3.1Prostate cancer progression occurs through three stages initiation, progression, and advancement. Prostate carcinoma is a multistep phenomenon where lesions develop in luminal epithelial cells to form new cells (Prostatic intraepithelial neoplasia (PIL)), PIL of the high grade was genetically similar to prostate carcinoma such as overexpression of BCL2, GSTP1, ki-67 and under expression of p27, PTEN, NKX3.1 [61]. Prostate cancer metastasizes to bone, liver, lungs, and lymph nodes with altered AR, PI3K, DNA repair, and TGF-β/SMAD4 pathways [66]. PC3 cells are derived from metastasized bone tumors. LNCaP cells were derived from metastasized lymph node tumor [67].

4.2.7 Signaling pathways in prostate cancer

Prostate gland development occurs through complex multiple pathways and involves the coordination of autocrine, paracrine, and juxtacrine signaling. Prostatic development occurs through determination, initiation, branching, differentiation, and maturation [68]. The major pathways that promote prostate cancer development and progression include androgen receptor (AR) signaling, NFκB signaling; Growth factor signaling (growth factors include Adrenomedullin, Angiopoietin, Autocrine Motility Factor, Bone Morphogenetic Protein, Brain-Derived Neurotrophic Factor, Epidermal Growth Factor, Erythropoietin, Fibroblast Growth Factor, Growth Differentiation Factor, Hepatocyte Growth Factor, Insulin-like Growth Factor, Nerve Growth Factor, Platelet-Derived Growth Factor, Transforming Growth Factorb, Tumour Necrosis Factor-α, Vascular Endothelial Growth Factor, Placental Growth Factor); Phosphoinositide-3-kinase/AKT signaling, Janus Kinase/signal transducers and activators of transcription (JAK/STAT) signaling, Mitogen-activated protein kinase (MAPK) Pathway, Wnt/β-catenin signaling [69-71] Fig. 10.

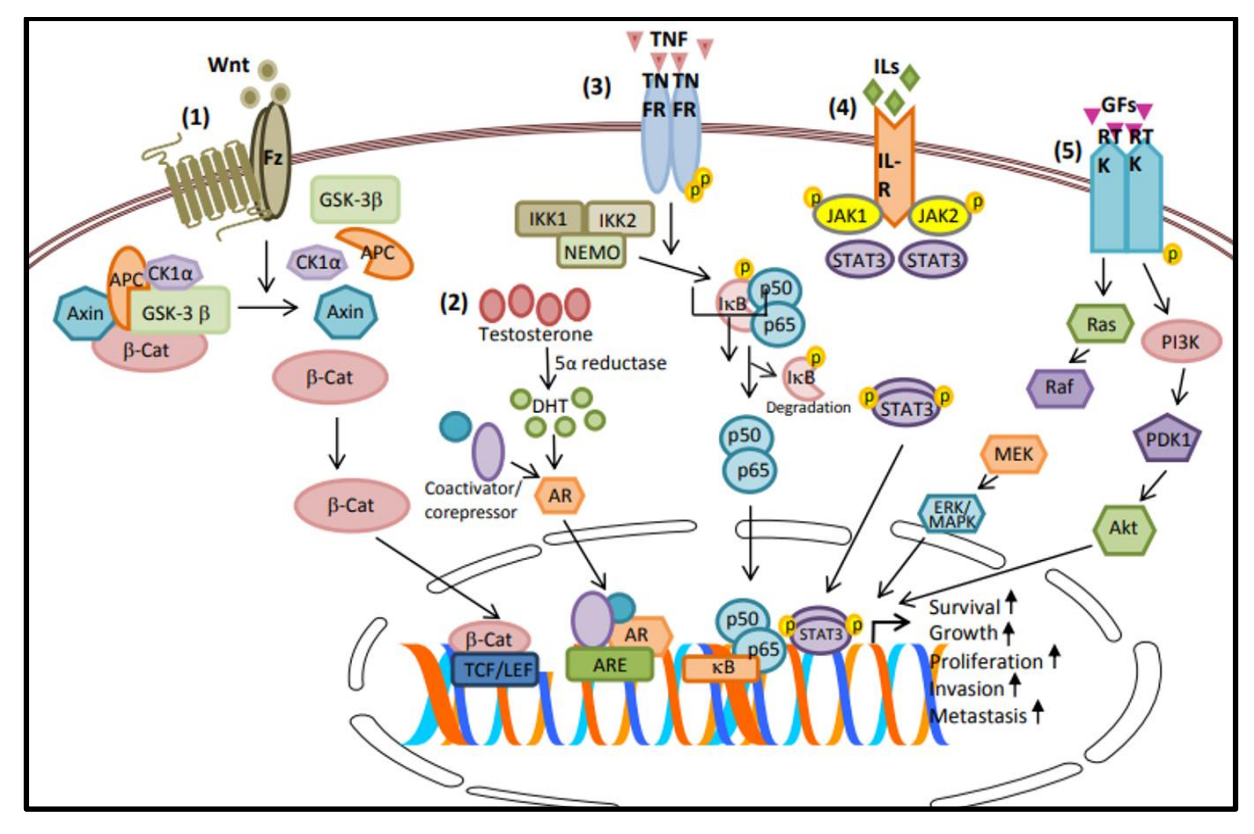


Fig. 10: Signaling pathways (androgen-independent) in prostate cancer (Adapted from [72]). Prostate cancer progression occurs through various signaling pathways such as Wnt/β-catenin, JAK/STAT, PI3K/Akt, Growth factor, NFκB, and MAPK signaling pathways inside the cell for cell survival, cell growth, cell proliferation, cell invasion, and metastasis.

4.2.8 Risk factors and medication

Hormones, advanced age, dietary fat, and hereditary genes were the risk factors for prostate cancer. Prostate cancer risk can be reduced due to either vitamin E or selenium supplements, soy proteins, medicines such as 5-alpha reductase inhibitors (finasteride, dutasteride), and aspirin [73] Fig. 11D. Some of the approved drugs for prostate cancer include Abiraterone acetate (Zytiga) (CYP17 inhibitor), MDV3100 (Enzalutamide) (Androgen-receptor (AR) antagonist), VN/124-1 (Galaterone) (Androgen receptor antagonist, AR degradation, CYP17 inhibition), Cabazitaxel (Microtubule inhibitor), Docetaxel (Microtubule inhibitor), Ixabepilone (Antimicrotubular agent), RAD-001 (Everolimus) (mTOR inhibitor), Dasatinib (Tyrosine kinase inhibitor), Saracatinib (Dual kinase inhibitor (Src and Bcr-Abl tyrosine-kinase inhibitor)), Denosumab (RANKL inhibitor) [69] Fig. 11C.

4.2.9 Detection, stages and treatment

Symptoms of prostate cancer include urination problems, blood in urine or semen, erectile dysfunction, weakness, or numbness in the legs. Prostate cancer can be detected either by testing the levels of PSA (normal-4 ng/ml) or by a digital rectal exam [74]. PSA levels the grade of cancer and tests used to detect prostate cancer include prostate biopsy (Gleason score), genetic testing, and imaging tests such as PET scan, MRI, CT scan, bone scan, Trans ultrasound, and lymph node biopsy. Staging of cancer was done and categorized into (i) primary tumor (category T (Tumor)) may be clinical (cT) or pathological (pT); (ii) spread to lymph node (category N (Node)), and (iii) spread to other parts of the body (category M (Metastasis)). Stage grouping of various categories done to detect the stage of cancer and includes from stage I to stage IV (Stage I (Gleason score 6, PSA less than 10)), Stage II (Gleason score 6-8, PSA in between 10-20), Stage III (Gleason score 8-10, PSA 20)), Stage IV (Any grade, Any PSA) [60]. With the advancement of new treatment technologies and the development of new drugs systemic therapy is gaining importance and various treatments are employed to reduce the further spread of disease [75]. Stage I treatment is given either by radical prostatectomy or by radiation therapy, Stage II treatment is done by radiation therapy, radical prostatectomy, hormonal therapy, and brachytherapy. Stage III treatment is performed by using external beam radiation with hormonal therapy, radical prostatectomy, Stage IV treatment by hormonal, external beam radiation, chemotherapy, surgery

(http://www.mpuh.org/centreforroboticsurgery/tag/different-stages-of-prostate-cancer/) **Fig.11A,B** .

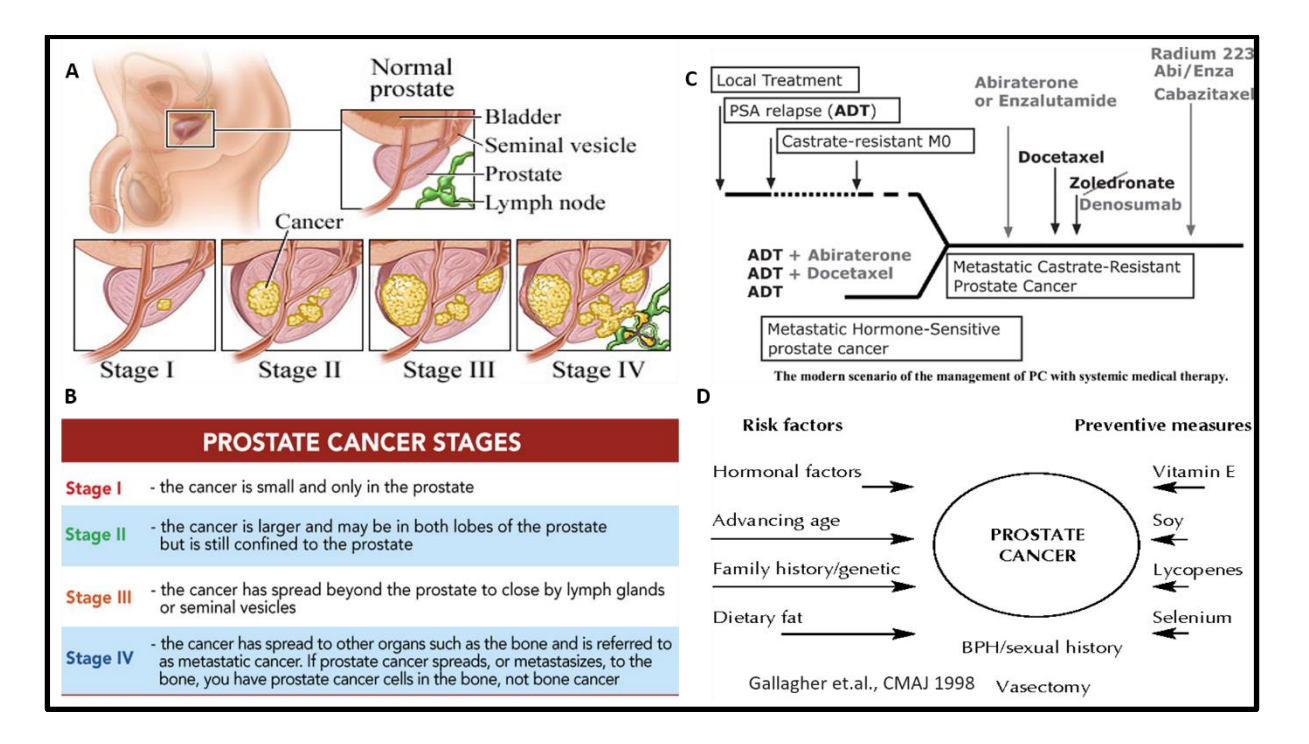


Fig. 11: Prostate cancer stages and treatment. Prostate cancer is of four stages and in each stage, cancer spreads to other lobes and to other tissues. Systemic therapy is widely used for the treatment of prostate cancer. A) Stages of prostate cancer. B) Description of each stage. C) Systemic therapy for prostate cancer. D) Risk factors and preventive measures for prostate cancer.

4.3 Methodology followed for objective I

4.3.1 Cell lines used for the study and growth condition

HEK293T, HeLa, DU145 & PC3 cells had obtained from ATCC. All these cells were maintained in DMEM supplemented with 10% Fetal Bovine Serum (FBS), 100 U/ml Penicillin, and 100 μg/ml Streptomycin and were cultured in 5% carbon dioxide (CO₂) & 37⁰c.

4.3.2 Plasmids used in this study

ECSIT gene had obtained from Harvard Medical School, the USA in a plx304 vector with clone id <u>HsCD00414947</u>. Histidine tag ECSIT was generated by sub-cloning from plx304+ECSIT Plasmid into PET28a(+) vector (gift from Dr. Naveen) through a traditional cloning procedure. The subclones used in this study include PET28a+ECSIT wild type, PET28a+ECSIT C43A, PET28a+ECSIT C21,43A, PET28a+ECSIT C14,21,43A, pEGFPN1+ECSIT & pEGFPN1+ECSIT C14,21,43A

4.3.3 Ribose nucleic acid (RNA) isolation

RNA was isolated as per the standard protocol, where the cells after reaching confluency washed with 1XPBS. The cells were resuspended with trizol and incubated in ice for 5 minutes; to this one-fourth volume of chloroform was add incubated for 10 minutes at room temperature. The solution was mixed and centrifuged at 12,000 rpm for 20 minutes at 4°c. The upper aqueous layer was collected into another tube and mixed with a half volume of isopropanol then incubated at room temperature for 10 minutes. Centrifugation had done at 12,000 rpm for 10 minutes at 4°c, the supernatant was discarded and the pellet was washed with 70% ethanol by centrifuging at 10,000 rpm for 5 minutes at 4°c. Discard the supernatant and air dry the pellet and resuspend in DEPC water. The RNA was converted to cDNA for further use [76, 77].

4.3.4 Quantitative real time Polymerase Chain Reaction

Quantitative real-time PCR had done according to manufacturing protocol (Bio-Rad). Reverse transcription PCR was performed using gene-specific primers using cDNA as template and mRNA levels were normalized using GAPDH as an internal control. Fluorescence intensity levels were measured using the Bio-Rad CFX94 system.

4.3.5 Generation of ECSIT knockdown cell line

Short hairpin RNA clones targeting specific gene (ECSIT) transfected to HEK293T cells using standard protocol and virus generated in the spent medium after 24h of transfection infected to cells where gene had to be knocked down (DU145, PC3) and kept for selection using puromycin antibiotic. Selected cells check using reverse transcription PCR and western blotting which proceeded further [78].

4.3.6 Cell proliferation / Cell viability assay

Cell viability or cell proliferation was checked using an MTT reagent. Seed the cells in 96 well plates (5000 cells) and incubate for 24hrs @ 37°c. Transfect with respective plasmids in wells and incubate for more 24hrs and MTT reagent (5mg/ml) 20µl added and incubated for 4hrs @ 37°c in dark. Remove the medium and add 200µl DMSO then measure the Optical Density @ 570nm using a microplate reader (Molecular devices- spectra max M2) [79].

4.3.7 Fluorescence activated cell sorting (FACS)

The stage-specific cell cycle analysis was done using FACS, which was detected using propidium iodide stain. Cells were harvested for the experiment and they were treated with nocodazole and thymidine at concentrations of 100ng and 2mM respectively. Cells were washed with 1xPBS and fixed with 70% ethanol in ice for 30 minutes. Fixed cells were stained with propidium iodide buffer (1XPBS + RNase A (50µg/ml) + PI (50µg/ml)) for 45 minutes in dark. Once the incubation had done cells were run on FACS Calibur machine acquisition and analyzed on an FL2A channel with a linear scale. The data plotted in FlowJo software and peaks obtained were taken [80].

4.3.8 Treatment and cell cycle synchronization

Cell cycle analysis had done by treating DU145 and PC3 cells with Nocodazole and thymidine. Nocodazole blocks the cells in the G2-M phase while thymidine blocks the cells in the G1-S phase. Cell cycle synchronization had done with nocodazole at 100ng/ml for 16h whereas Thymidine synchronization had done at 2mM. RNA was isolated and quantitative RT-PCR was used to verify the expression of mRNA levels, protein lysates were generated, and western blotting was used to detect the stage-specific cyclin expression. The efficiency of synchronization had done by running the samples using a flow cytometer [81].

Results

5.1 ECSIT expression levels were found to be high in prostate cancer

ECSIT plays an important role in Infection, Mitophagy, Immunity, and Aging, and the effect of this function was seen in cancer cells. Since interacting partners of ECSIT responsible for these functions had a role in cancer progression, thus we hypothesize that ECSIT might participate in cancer. To explore its new role, we screen the cancer atlas database and observed that its RNA expression was higher in prostate cancer than in other malignancies. Similarly, immunohistochemistry (IHC) data **Fig. 12** from the protein atlas database reveals that its protein expression is high in prostate cancer when compared to others.

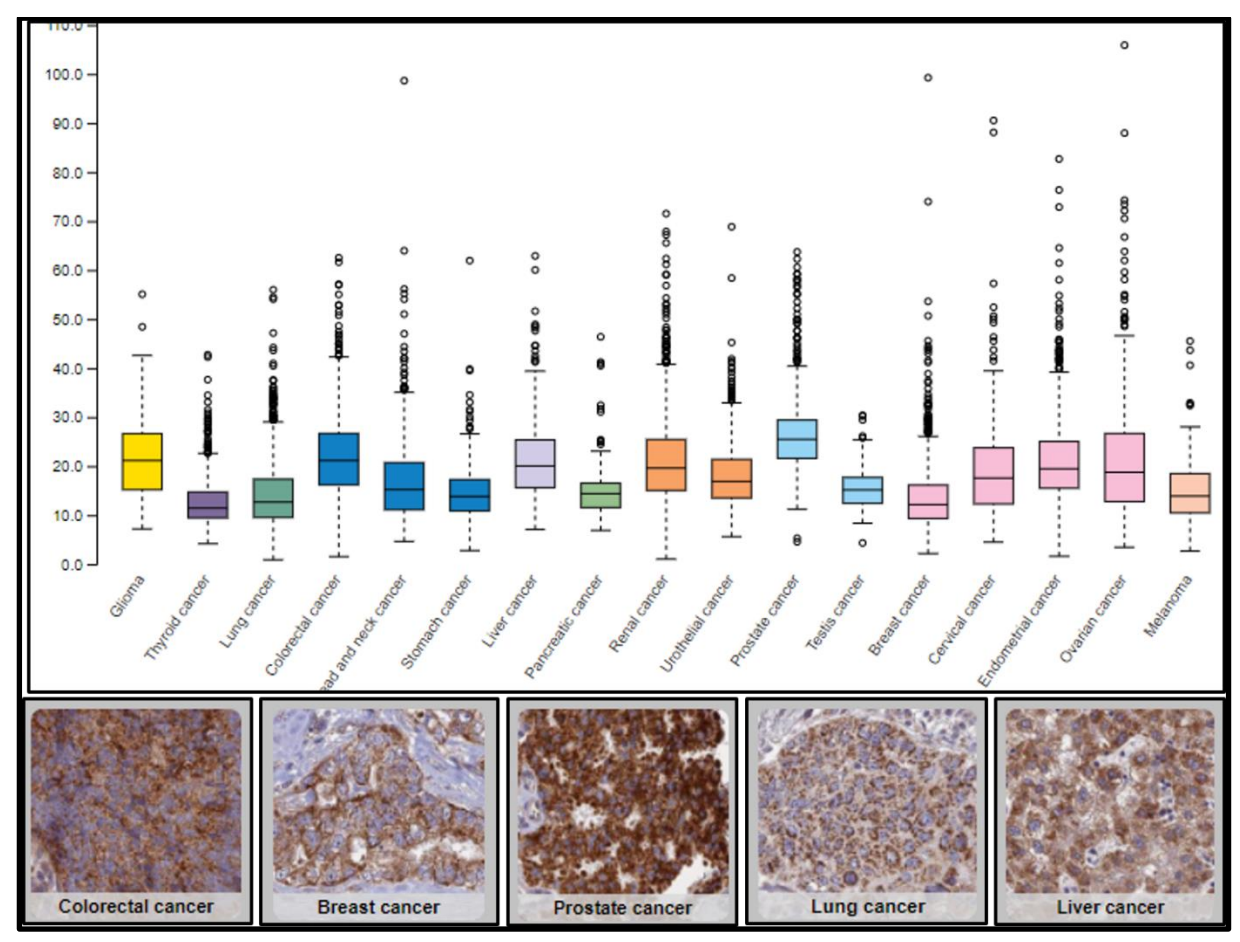


Fig. 12: ECSIT expression was found to be high in prostate cancer. mRNA expression of ECSIT in various cancer cell lines as seen in the protein atlas database and the maximum was found to be highest in prostate cancer followed by glioma, colorectal, liver, etc... Similarly, the immunohistochemistry images show the protein expression of ECSIT was high in prostate cancer.

5.2 Abrogation of ECSIT reduces the proliferation and survival of prostate cancer cells

The functionality of protein is examined by knockdown or overexpression studies. To test the function of ECSIT in prostate cancer cells we used a lentivirus knockdown strategy with three targets **Fig. 13A**, **C**. The microscopic observation of ECSIT cells with lentivirus knockdown and their respective controls revealed that targets 1 and 3 showed reduced proliferation in DU145 cells whereas target 3 showed reduced proliferation in PC3 cells **Fig. 13D**. The reduced number of cells led to a suspicion that the survival rate might be hampered. In order to check the survival rate of knockdown cells, a cell viability assay using MTT was done for 24h, 48h, and 72h after seeding an equal number of cells in 96 well plate and it was observed that in DU145 reduced survival in target 1 whereas in PC3 reduced survival rate in target 3 after 72 hours **Fig. 13B**. This confirms that the knockdown of ECSIT reduces the proliferation and survival capacity of cells in comparison with the control.

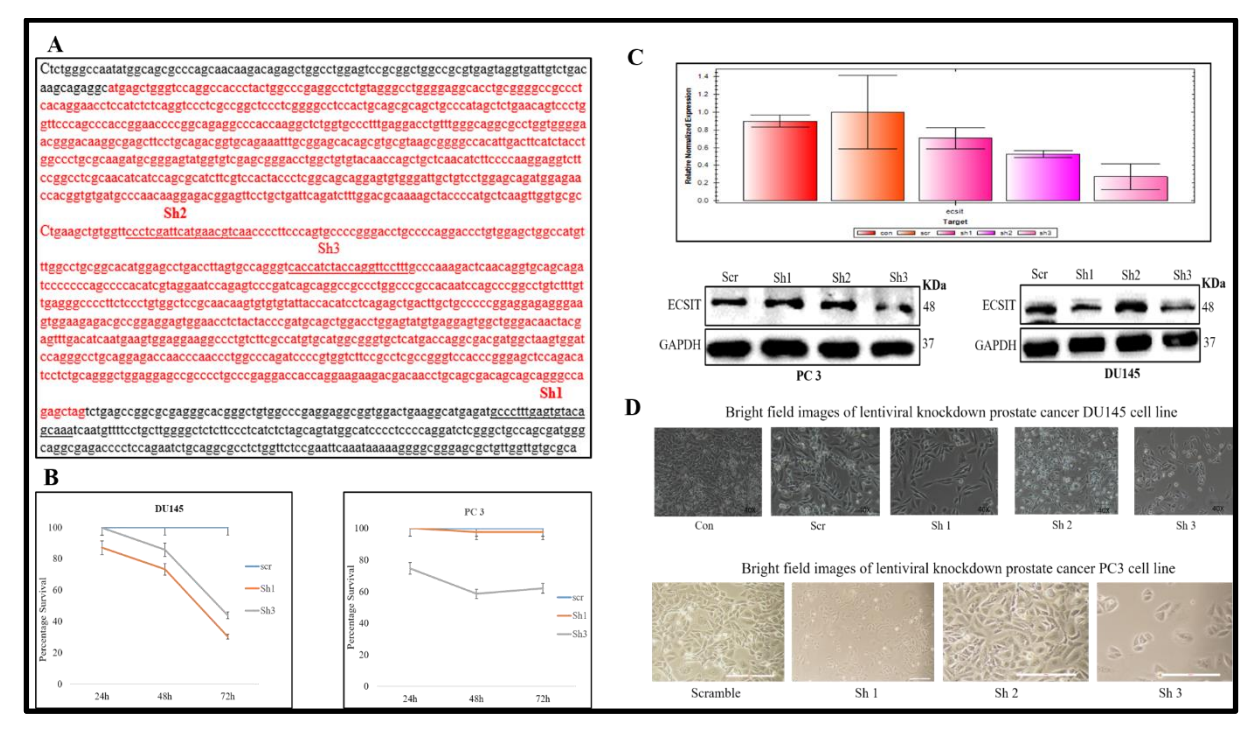


Fig. 13: ECSIT knockdown shows less cell proliferation & survival rate. A) Lentivirus targeting sites were shown on the ECSIT gene. The red color indicates the coding region. B) Cell viability assay using MTT in DU145 & PC3 cells. C) Validation of knockdown using RT-PCR & western blotting. D) Bright-field images of various lentivirus targets in DU145 and PC3 cells. Error bars were represented by taking the standard error mean of triplicate values.

5.3 ECSIT Knockdown displays delayed cell cycle progression.

In comparison with the scrambled, knock-down, cells have lower cell growth and survival rates. Because the cell proliferation rate is dependent on coordinated cell cycle regulation, we suspect that ECSIT may play a role in cell cycle regulation. To elucidate the mechanism, we synchronized the cells with nocodazole and released them for various time points. The results reveal that synchronized control cells took 12hrs to reach the G2 phase, whereas knockdown cells took 20h in PC3 cells **Fig. 14A**, **B**. To ensure the cell cycle markers were in correlation with our FACS data we performed western blotting with all cyclins and the results confirmed that varied expression levels of cyclin E in knockdown cells upon comparison with control in DU145 and PC3 cells **Fig. 14D**, **F**. This provides further evidence that delayed cell cycle at the G1-S phase transition is due to the knockdown of ECSIT the in both cell lines **Fig. 14C**, **E**.

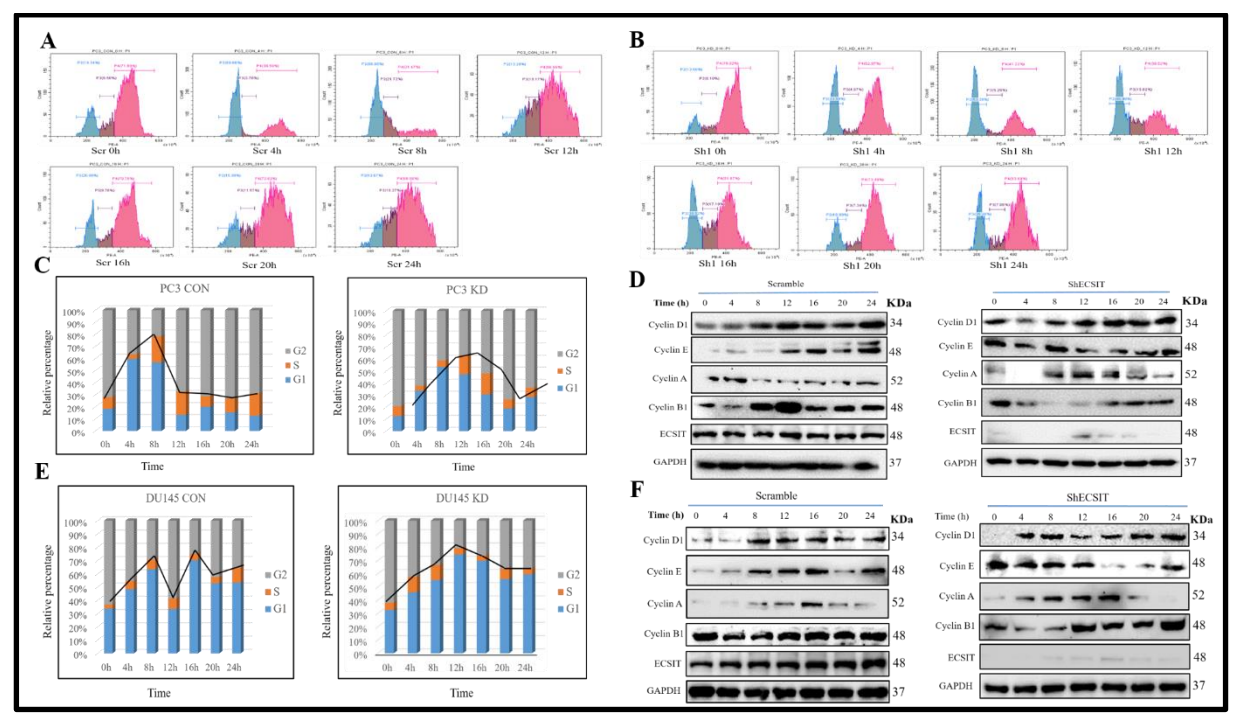


Fig. 14: ECSIT shows less proliferation rate due to either JAK/STAT or HIPPO/YAP signaling in DU145 cells. (A, B) FACS data for nocodazole synchronization of PC3 cells. (C) Percentage of cells in various phases for PC3 cells. (D) Western blotting data of marker proteins for PC3 cells. (E) Percentage of cells in various phases for DU145 cells. (F) Western blotting data of marker proteins for DU145 cells.

5.4 The delay in the cell cycle was due to altered proliferative cell signaling

It was revealed from the above set of experiments that ECSIT through cyclin E plays a role in cell cycle progression. Since cyclins are under the control of various upstream signaling pathways, we then tested various signaling pathways, which are known to regulate the proliferative signals in prostate cancer. Literature studies reveal proliferation in DU145 cells occurs through JAK/STAT and HIPPO/YAP signaling pathways. Therefore, we then did a western blot for JAK/STAT and HIPPO/YAP pathway markers. The results showed that phospho JAK at tyrosine 221 and phospho STAT at tyrosine 705 levels were reduced only in ECSIT knockdown DU145 in comparison with other phosphoproteins in JAK/STAT pathway Fig. 15A. When we looked at the HIPPO/YAP pathway, we observed that phospho YAP at serine 127 was lower in both DU145 and PC3 knockdown cells than in controls (Fig. 15B, C). By altering signaling pathways in DU145 and PC3 cells, we identified a putative role of ECSIT in prostate cancer. Therefore, these results conclude that ECSIT regulates the proliferation of DU145 cells under JAK/STAT & HIPPO/YAP pathway whereas, PC3 cells proliferate under HIPPO/YAP pathway.

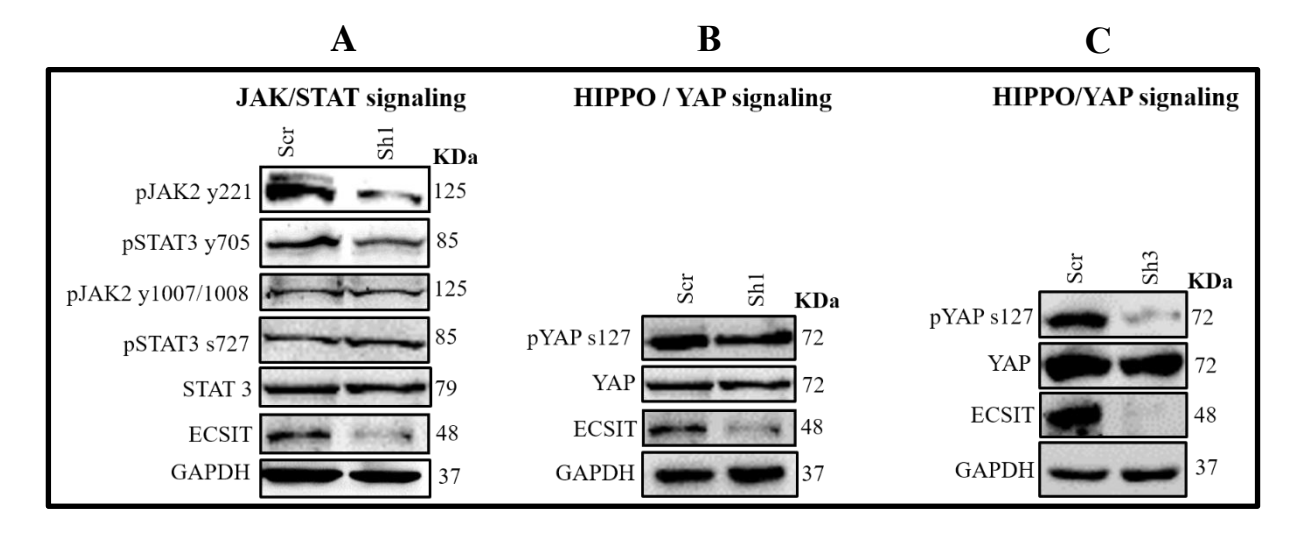


Fig. 15: Hampered Molecular Signaling Pathways under ECSIT knockdown. (A, B) The reduced proliferation of DU145 cells was due to reduced phosphorylation of JAK at tyrosine 221 and for STAT at tyrosine 705 whereas in HIPPO/YAP, pathway phosphorylation at serine 127 was found to be reduced under ECSIT knockdown. (C) The reduced proliferation of PC3 cells was due to reduced phosphorylation at serine 127 under ECSIT knockdown.

5.5 Cell survival and cell death pathways were altered under ECSIT knockdown conditions

The homeostatic role of ECSIT in prostate cancer cells was evident from previous observations and it was predicted to act as a balance between cell death and survival pathways. We then wanted to decipher the cell death pathways in ECSIT knockdown DU145 & PC3 cells. Western blot data of marker proteins reveals that ECSIT knockdown in DU145 cells shows enhanced autophagy whereas, ECSIT knockdown in PC3 cells shows enhanced apoptosis **Fig. 16A, B, D, E.** Since, mTOR regulates autophagy under the control of AKT, ERK, and AMPK mediates signaling. Our analysis in DU145 cells shows reduced levels of mTOR along with their upstream kinases such as MEK and ERK with concomitant upregulation of downstream effectors i.e., ATG5, ATG 16L leading to autophagy **Fig. 16C.** In PC3 knockdown cells increased apoptosis was observed. Our further analysis revealed that PI3K/Akt signaling enhanced the intrinsic apoptosis pathway that leads to apoptosis in ECSIT knockdown PC3 cells compared to scramble **Fig. 16F.** Therefore, these results conclude that silencing of ECSIT resulted in the activation of PI3K/Akt signaling leading to enhanced intrinsic apoptosis of PC3 cells. The summary of autophagic or apoptotic cell death leading to reduced proliferation was shown in **Fig. 16G.**

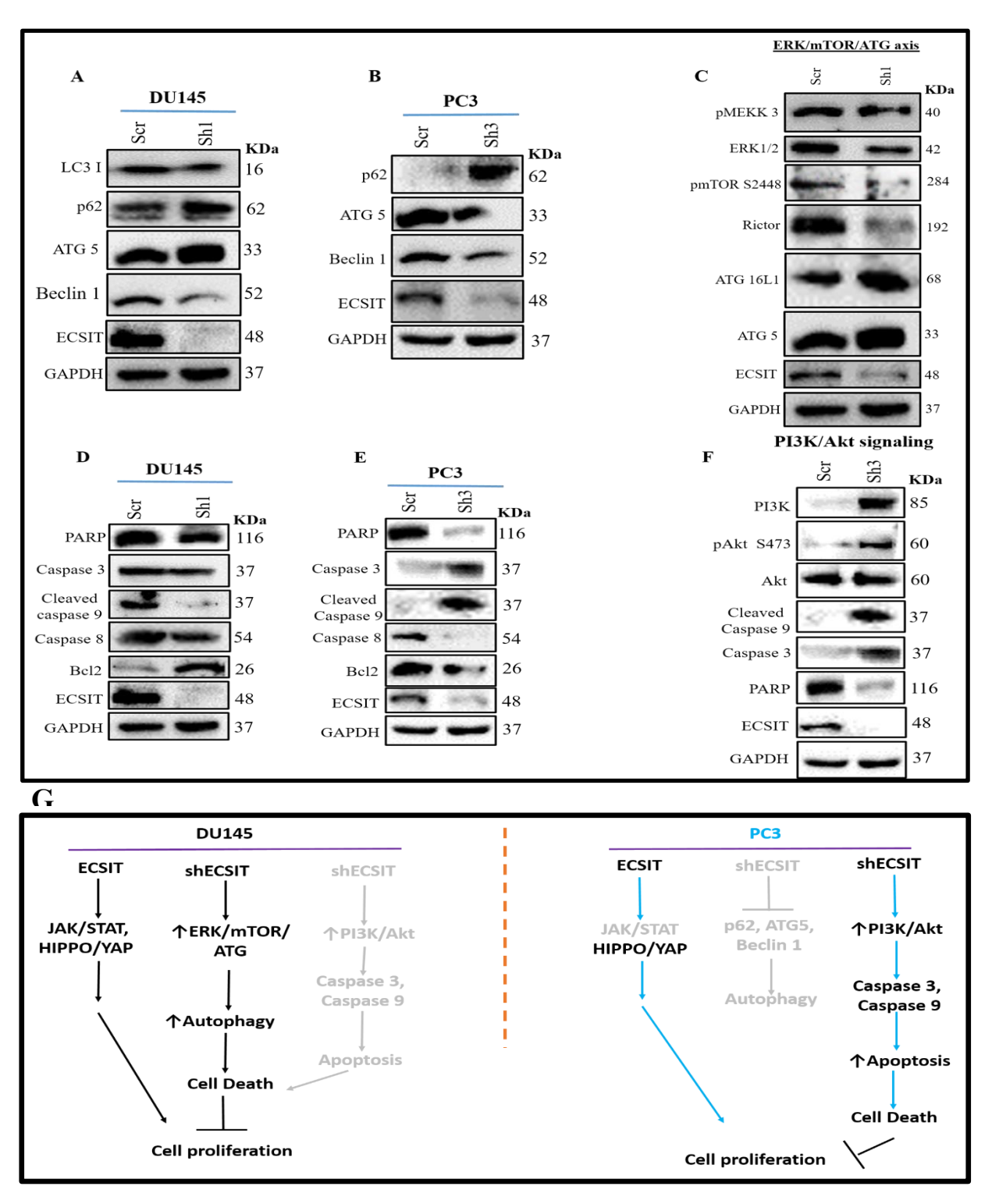
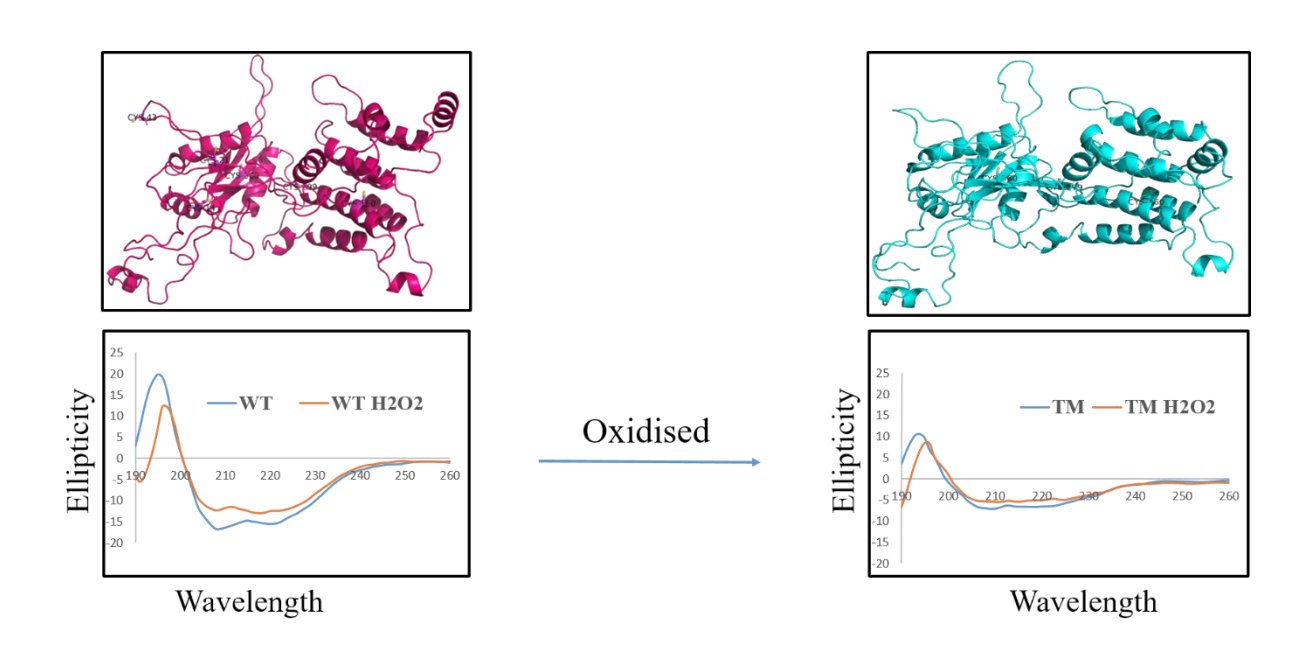


Fig. 16: Ablation of ECSIT attenuates tumorigenesis either by apoptosis or autophagy in prostate cancer cells. (A, B) Western blotting data of autophagy marker proteins in DU145 & PC3 cells reveal enhanced autophagic cell death as observed through autophagy marker proteins such as ATG5, p62 & LC3 in DU145 cells. (C) The molecular mechanism of autophagy in DU145 cells depicts a reduced ERK/mTOR/ATG axis under the knockdown condition in DU145 cells. (D, E) Western blotting for apoptosis marker proteins in DU145 &

PC3 cells reveals enhanced apoptosis as observed through apoptotic marker proteins such as Caspase3, Bc12 & PARP in PC3 cells. (F) The molecular mechanism of apoptosis in PC3 cells depicts reduced PI3K/Akt signaling proteins under the knockdown conditions in PC3 cells. (G) Summary of autophagic & apoptotic cell death in DU145 & PC3 cells.

Objective II: Characterisation of ECSIT: *Insilico* and *in-vitro* approach



6.1 Introduction

Cells are prone to various stressors in our daily life and they try to cope by producing antioxidants, which defend them. The oxygen-bearing compounds, which were produced inside the cells either due to excessive metabolism or exposure due to irradiations, were known as reactive oxygen species (ROS). ROS include hydrogen peroxide, superoxide anion, alkoxy radical, hydroxyl radical, peroxy radicals, etc...ROS may have adverse effects such as lipid peroxidation, DNA damage, etc...ROS levels were maintained under basal levels in the normal cell due to the action of antioxidant enzymes that regulate them. ROS were produced inside the cell either due to the action of reduced nicotinamide adenine dinucleotide phosphate oxidase (NADPH oxidase) or by the electron transport chain system [82]. ROS levels were regulated by catalase, superoxide dismutase (SOD), peroxidases, etc...[83] The disturbed ROS may lead to an imbalance in the redox status of the cell thereby disturbing the homeostasis of the cell. ROS affects the cells through various signaling mechanisms inside the cell. Studies had shown that ROS at 10nM enhances cell proliferation, differentiation, migration, and angiogenesis; at the 100nM range shows inflammation and stress response whereas at the micromolar range arrests the growth of the cell and may lead to cell death [84].

ECSIT localizes to mitochondria and nucleus by possessing mitochondrial and nuclear localization signal sequence but it is a point to note under which circumstances this localization gets affected. Emerging evidence from recent reports provide us insights that Mitophagy occurs in response to stress [17] hence we predict mitochondrial localization was affected in response to stress. The cementing connection between ROS and partner-binding proteins provides us with a better understanding of ROS regulation, where the knockdown of partner-binding proteins elevates the ROS levels [85-88]. To unveil the role of ECSIT in ROS regulation, ROS levels were measured using DCFDA and this study explains the fact of negative correlation. For instance, the knockdown of ECSIT elevates the ROS levels and vice versa hence, we confirm abrogation of ECSIT aggravates ROS levels. Significance of localization of various factors [89-91] posed us a query regarding the localization of ECSIT under oxidative stress. The localization of ECSIT is hampered by inhibiting the partner binding interactions through proteins such as PRDX1 [25], PRDX6 [10], CRBN [37], p62 [36] upon screening TRAF6 interacting domains it was revealed that PRDX6 and ECSIT share a similar domain with TRAF C domain of TRAF6. Therefore, we hypothesize interactions of privileged interactions on ECSIT, with TRAF6 or PRDX6 determine its perspicuous role Fig. 17.

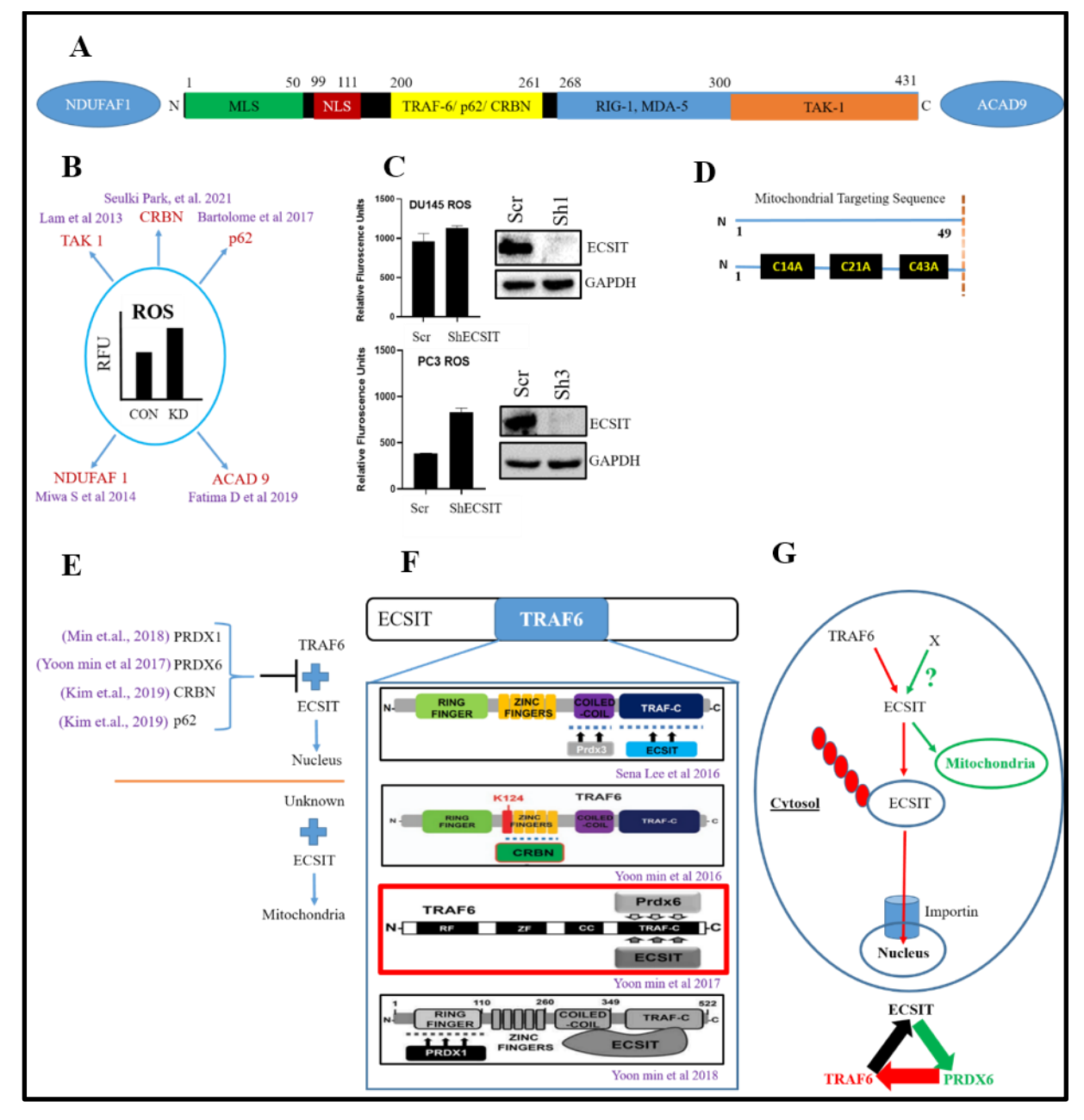


Fig. 17: Privileged interaction on ECSIT determines its perspicuous role. (A) Domain structure of ECSIT with its partner binding regions. (B) Knockdown of partner binding proteins aggravates ROS. (C) Knockdown of ECSIT aggravates ROS. (D) Wild type & Mutant N-terminal cysteines on mitochondrial targeting sequence. (E) Inhibition of co-localization by PRDX1, PRDX6, CRBN & p62. (F) Interaction of inhibitory proteins on TRAF6. (G) Partner-specific interaction on ECSIT affects its co-localization.

6.2 Materials used and methodology followed for objective II

6.2.1 Cell lines used for the study and growth condition

HEK293T, HeLa, DU145 & PC3 cells had obtained from ATCC. All these cells were maintained in DMEM supplemented with 10% Fetal Bovine Serum (FBS), 100 U/ml Penicillin, and 100 μg/ml Streptomycin and were cultured in 5% carbon dioxide (CO₂) & 37⁰c.

6.2.2 Plasmids used in this study

ECSIT gene had obtained from Harvard Medical School, USA in plx304 vector with clone id HscD00414947. Histidine tag ECSIT was generated by sub cloning from plx304+ECSIT Plasmid into PET28a(+) vector (gift from Dr. Naveen) through traditional cloning procedure. The sub clones used in this study include PET28a+ECSIT wild type, PET28a+ECSIT C43A, PET28a+ECSIT C21,43A, PET28a+ECSIT C14,21,43A, pEGFPN1+ECSIT, pEGFPN1+ECSIT C14,21,43A.

6.2.3 Reagents used in this study

A detailed list of reagents along with their catalogue used in this study were mention in below Table 4.

Table 4: List of reagents used.

S.No.	Name of the reagent	Catalogue
1.	0.25% Trypsin- EDTA (1X)	25200072-500ml
2.	Acetic acid glacial	10010-500ml
3.	Acrylamide	1610107-1KG
4.	Ammonium Persulfate	1610700-10G
5.	Ampicillin Sodium salt	CMS645-5G
6.	Anti-Anti (100X)	15240062-100ml
7.	Benzonase nuclease	E1014-5KU
8.	Bovine serum albumin	MB083-25G
9.	Calcium chloride dihydrate	C7902-500G
10.	Cell culture plates and dishes	Eppendorf
11.	Charcoal activated powder	MB261-250G
12.	Chloroform	10470-500ml
13.	DAPI	P36931
14.	DCFDA	D399
15.	Dimethyl sulphoxide	70620-500ml
16.	DL-Dithiothreitol	43815-1G
17.	Dulbecco's Modified Eagle Medium	12100046
18.	EcoRI	R0101S
19.	EDTA	E6758-100G
20.	EGTA	E-8145
21.	Ethidium Bromide	054817

24. Formaldehyde 70710-2 25. Glycine MB013 26. Hard shell PCR plates 96-well HSP960 27. HEPES H4034- 28. Hexylene glycol 112100 29. Hind III R0104S	3-500G 01 -25G -500G S
24. Formaldehyde 70710-2 25. Glycine MB013 26. Hard shell PCR plates 96-well HSP960 27. HEPES H4034- 28. Hexylene glycol 112100 29. Hind III R0104S	500ml 5-500G 01 -25G 500G S
25. Glycine MB013 26. Hard shell PCR plates 96-well HSP960 27. HEPES H4034- 28. Hexylene glycol 112100 29. Hind III R0104S	3-500G 01 -25G -500G S
26. Hard shell PCR plates 96-well HSP960 27. HEPES H4034- 28. Hexylene glycol 112100 29. Hind III R0104S	01 -25G -500G S
27. HEPES H4034- 28. Hexylene glycol 112100 29. Hind III R0104S	25G -500G S 9-100G
28. Hexylene glycol 112100 29. Hind III R0104S	-500G S 9-100G
29. Hind III R0104S	S 9-100G
	9-100G
30. Hydrogen peroxide H1009	
	2-25G
32. Isopropyl-β-D-thiogalactopyranoside MB072	230
33. Lipofectamine 2000 52887	
34. Kanamycin sulphate TC136-	
35. Luria Bertani Agar M1151	
36. Luria Bertani Broth M1245	
37. MTT RM113	
38. N,N'-Methylene bis (acrylamide) 146072	-500G
` ' 1	387-500G
40. Nitrocellulose membrane 0.45μm 162011	5
41. Nocodazole M1404	-2MG
42. Opti MEM (1X) 319850	70
43. Phenol saturated 162416	2-500ml
44. Phenylmethanesulfonyl fluoride (PMSF) P7626-3	5G
45. Ponceau S P3504-	10G
46. Potassium Acetate 164918	6
47. Potassium chloride RM698	s-500G
48. Propan-2-ol 71390-3	500ml
49. Propidium iodide P4170-2	25MG/
P4864-	10ml
50. Puromycin dihyrochloride TC198-	-25MG
51. Q5 DNA polymerase M0491	S
52. RNA isoplus 9109-20	00ml
53. Seakem LE Agarose 50004-5	
54. Sodium azide S2002-	100G
55. Sodium bicarbonate S5761-:	
56. Sodium chloride MB023	5-5KG
57. Sodium phosphate dibasic anhydrous (Na ₂ HPO ₄) MB024	—250G
58. Sodium phosphate monobasic anhydrous (NaH ₂ PO ₄) GRM39	964-500G
59. T4 DNA ligase EL0014	1/M0202S
60. TEMED 161080	-50ml
61. Tergitol solution NP40S-	-100ml
62. Tert-butyl Hydro peroxide B3153-	100g
63. Thymidine T1895-	1G
64. Trans-1,4-Dimercaptobutane (SDT) BD126	893
	7-500G
66. Triton X-100 93443-	
67. XhoI R0146S	

6.2.4 In-silico prediction of ECSIT mitochondrial localisation

It was suspected that the ECSIT protein, which was translocated to mitochondria [6], possessed a mitochondrial signal sequence. MitoprotII server reveals it translocate to mitochondria with a score of 0.99 at the N-terminus region **Fig. 18**. N-terminus signal sequence spans from amino acid 1-49. DeepMito web server reveals it translocates to the mitochondrial inner membrane with a score of 0.24 **Fig. 19**.

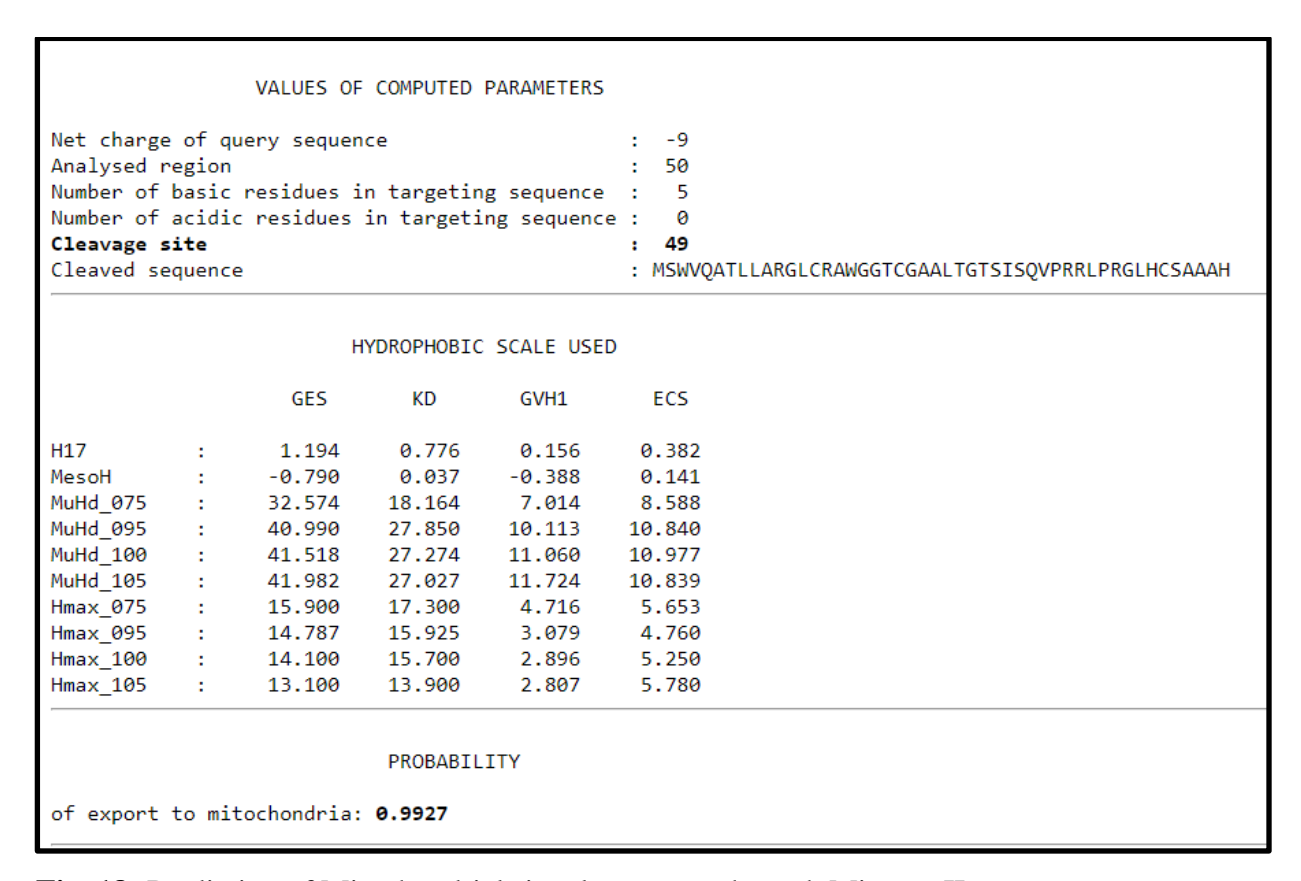


Fig. 18: Prediction of Mitochondrial signal sequence through MitoprotII server.



Fig. 19: Prediction of subcellular localisation through DeepMito webserver.

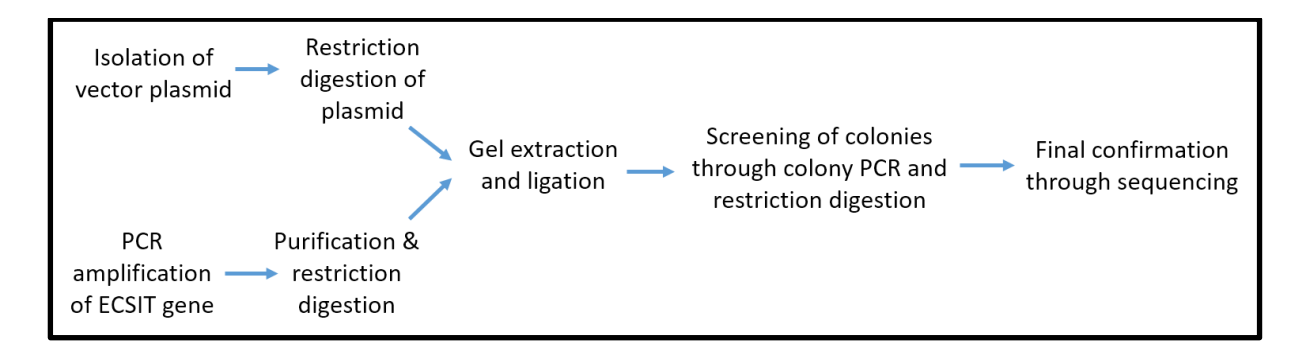
6.2.5 Three-dimensional (3D) structure and molecular dynamics simulation of ECSIT

The three-dimensional structure of human ECSIT was fetched from the Alpha Fold, which was available through uniprot database (Uniprot: Q9BQ95). The structure obtained from Alpha fold was subjected to molecular dynamics (MD) simulation for further refinement. The MD simulation was carried out using GROMACS 2020.6 package installed on a Linux cluster. The CHARMM-36 (an all-atom force field) was used to parameterize the protein. The Alpha Fold structure was placed in a cubic box with TIP3P water models and 150mM NaCl was added to maintain the electrical neutrality of the system. Before proceeding to MD simulation 2500 cycles (with step size 1ps) steepest descent-based energy minimization was carried out to relax the system and minimize any close contacts. Then the system was heated at 300K using a Berendsen thermostat (with 0.1ps of thermal coupling) under NVT ensemble for 100ps. Further 100ps equilibration was carried out under the NPT ensemble during all the equilibration the bonds were restrained using the LINCS algorithm. The structure obtained at the end of the NPT simulation was passed to the MD simulation, for 250ns, under the NPT ensemble. During the entire simulation, the long-range interactions were computed through the Particle-mesh Ewald method, and the van der Waals interactions through cut-off (for electrostatic and nonelectrostatic respectively), all these non-bonded interactions were calculated over 10Å. Post-MD simulation the cluster analysis was carried out to obtain the best structure of ECSIT, and this was referred to as the refined 3D structure of ECSIT. Further, the refined structure of ECSIT was subjected to 100ns of MD simulation to obtain the best wild-type structure. Then the N-terminal cysteines (Cys 14,21,43) were modified to alanine and this structure was again subjected to 100ns MD simulation. A similar methodology was followed as detailed above [92]. Both wild-type and N-terminal mutant structures were subjected to protein-protein docking, using ClusPro 2.0 server, with PRDX6, TRAF6, and TOM20.

6.2.6 Molecular cloning (Traditional)

ECSIT was commercially obtained from Harvard University in plx304 vector and subcloned into pET28a+, pEGFPN1 vectors. Sub-cloning of ECSIT was done using the traditional cloning method where empty vectors were isolated as plasmid by alkaline lysis method, ECSIT was PCR amplified, and restriction digestion was performed using XhoI, EcoRI enzymes for pEGFPN1 and EcoRI, Hind III for pET28a+. Digested products were run on agarose gel and purified products ligated and transformed into XL-BLUE (gift from Dr. Naveen) host screened by using colony PCR, and restriction digestion which was finally confirmed using Sanger

sequencing (outsourcing - bio serve). The summary of the cloning procedure mentioned in the flowchart [93].



6.2.7 The polymerase chain reaction of cDNA amplification

Polymerase chain reaction performed according to the protocol suggested by New England Bio labs where reaction components (10X Standard Taq Buffer, 10mM dNTPs, 10 μ M Forward primer, 10 μ M Reverse primer, Taq Polymerase, Nuclease free water, Template DNA) were mixed individually and program set manually as suggested by NEB. The final PCR product had run on an agarose gel to check for amplification.

6.2.8 Site-directed mutagenesis (SDM)

Site-directed mutagenesis (SDM) is a procedure of generating gene variants specific to one particular amino acid. SDM includes various methods out of which the overlap PCR method is one among them. Here individual short and long fragments were PCR amplified individually and mixed in equimolar ratio as templates and run for a few cycles without final extension temperature and primers corresponding to wild type were added and run for a few more cycles and obtained mutant full-length product was digested, transformed, and screened using colony PCR, double digestion and sequencing [94]. The detailed methodology shown in Fig. 20.

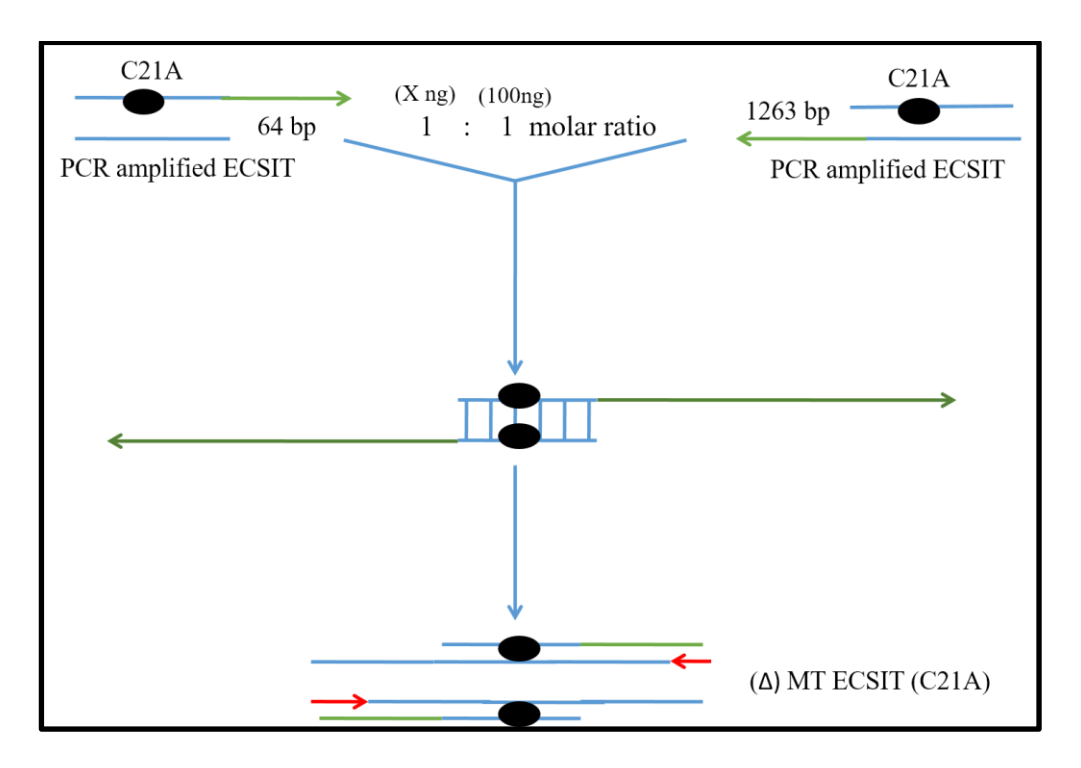


Fig. 20: Procedure for site-directed mutagenesis by overlap PCR method.

6.2.9 Agarose Gel Electrophoresis

The method of resolving biomolecules (nucleic acids) through size basis can be achieved through agarose gel electrophoresis. Agarose gel was prepared by dissolving agarose in 1X TAE buffer (50X TAE = Tris base, 0.5M EDTA PH 8.0, Acetic acid). The nucleic acid to be resolved is mixed with loading dye (6X loading dye= Sucrose, Bromophenol blue). The obtained bands were visualized through a UV trans illuminator (Major Science).

6.2.10 Transfection

The incorporation of double-stranded DNA into mammalian cells with the help of a lipid carrier is achieved through the transfection procedure. It is a method where DNA and Lipofectamine 2000 (reagent) are diluted individually in an OptiMEM medium and incubated for 10 minutes. The individual complexes were mixed and incubated again for 30 minutes and add to cells. Cells had incubated for 24h and checked for the expression of protein either through a fluorescence microscope or through western blotting.

6.2.11 Protein Expression in prokaryotic host

The recombinant protein was expressed in expression host (arctic) cells containing the desired gene of interest was transformed and induced with 1mM IPTG concentration and cells were

precipitated under 8000rpm @ 4°c and lysed with lysis buffer (50mM Tris pH 7.5, 2mM EDTA,150mM NaCl, 2mM DTT, 200mM PMSF, 1mg/ml lysozyme). Complete lysis achieved through sonication (10sec on and 10sec off) and centrifuged under 14000 rpm @ 4°c. The obtained supernatant and pellet fractions were loaded onto the SDS gel to check for expression. Here protein was majorly found in pellet fraction and several strategies have been applied to obtain protein in supernatant some of them include a change in IPTG concentration, temperature, change of strain, co-transformation with chaperon plasmids, change of vector, etc. [95].

6.2.12 Protein Purification of His tag using Ni-NTA column

The expressed protein was purified using a Ni-NTA superflow cartridge (protocol suggested by Qiagen). This suggests the use of activation buffer NPI-10 (50mM NaH₂PO₄, 300mM NaCl, and 10mM imidazole) then loading of lysate into the column, and unbound protein washed with NPI-20 (50mM NaH₂PO₄, 300mM NaCl, 20mM imidazole). Finally, the remaining bound protein was eluted and collected separately using elution buffer NPI-250 (50mM NaH₂PO₄, 300mM NaCl, and 250mM imidazole). The collected fractions were protein estimated using the Bradford method and loaded onto the SDS gel to check the purity [96].

6.2.13 Immunoblotting

Immunoblotting had performed using protein isolated from the cells, which was run on the SDS-PAGE and then transferred to a nitrocellulose membrane, blocked with 5% skimmed milk, and probed with primary antibodies such as anti-ECSIT, anti-GAPDH, anti-IkBα, and anti-TRAF6. The unbound protein was washed with 1XTBST (1M Tris-HCl pH 7.5, 1M NaCl, 0.5% Tween 20) and re-probed with the corresponding secondary antibody (conjugated with HRP) again washed with TBST and developed using hydrogen peroxide as a substrate using chemiluminescence [10].

6.2.14 Oxidative stress

HEK-293T, HeLa cells grown in DMEM for 48hrs and treated with various concentrations of hydrogen peroxide (H₂O₂), tertiary butyl hydroperoxide (tBHP), and rotenone and protein were isolated from the cells and checked for expression using western blot [91].

6.2.15 Circular dichroism (CD)

Purified 50μg/ml protein was treated with or without H2O2 (oxidizing agent) with varying concentrations such as 0.5mM, and 1mM for 1h, and the secondary structure of CD spectra was recorded using Jasco-810 CD spectrophotometer in 190-300nm. The parameters used here were a 0.1cm path length cuvette, a data pitch of 0.1nm, and a scan speed of 100nm/min. Results were analyzed using sigma plot software and secondary structure predicted using dichrowebserver [97].

6.2.16 Fluorescence spectroscopy

Purified 50µg/ml protein was treated with or without H2O2 (oxidizing agent) or sodium dithionite (reducing agent) with varying concentrations such as 0.5mM, 1mM for 1h using an excitation wavelength of 280nm and emission wavelength of 290-410nm with a slit width of 8 and fluorescence intensities measured using a spectrophotometer [98].

6.2.17 Estimation of Reactive Oxygen Species using DCFDA

Cells after reaching confluency were washed with 1X PBS and trypsinized, centrifuged, and counted manually. Approximately 5000 cells were seeded in 96 well plates and incubated at 37c for 24h respective treatment or transfection was done and 20µm DCFDA was added, incubated for 1h, and fluorescence measurements were done at 492nm-517nm using a microplate reader (Molecular devices-spectra max M2) [99].

6.2.18 Immunofluorescence

HEK293T cells were seeded in a six-well plate with a coverslip once they reach 70% confluency they were transfected with GFP-ECSIT, MitoRFP (HeLa). Cells were washed with PBS, fixed with 4% paraformaldehyde for 20 minutes, and permeabilized with 0.1% Triton X-100 in 1XPBS (Nacl, Kcl, Na₂HPO₄, KH₂PO₄) for 5 minutes. Nuclei stained with DAPI with mounting media. Cells imaged on Zeiss LSM-170 laser confocal microscope [25].

6.2.19 Statistical analysis

All the statistical analysis were done using graph pad prism and densitometry graphs were plotted using Image J software.

6.2.20 Oligonucleotide used in this work

Oligonucleotide Sequences used for this study include lentivirus, real-time PCR, and for cloning of ECSIT in eukaryotic and prokaryotic vectors which were listed below tables.

Table 5: List of lentivirus sequences obtained from Dr. Gangisetty Subbarao Lab, Indian Institute of Science, India.

S.No	Gene name	Gene sequence	Validation
1.	ECSIT A11 (Sh1)	CCGGGCCCTTTGAGTGTACAGCAAACTCGAGTTTGCT	A549
		GTACACTCAAAGGGCTTTTTG	
2.	ECSIT A12 (Sh2)	CCGGCCCTCGATTCATGAACGTCAACTCGAGTTGACG	A549
		TTCATGAATCGAGGGTTTTTG	
3.	ECSIT B2 (Sh3)	CCGGCACCATCTACCAGGTTCCTTTCTCGAGAAAGGA	A3
		ACCTGGTAGATGGTGTTTTTG	

Table 6: Primers used for real time PCR.

S.No.	Target	Forward primer	Reverse primer
1.	ECSIT	GAGTTCCTGCTGATTCAGATCTTT	CAAAGGAACCTGGTAGATGGTGAC
2.	GAPDH	AGGTCGGAGTCAACGGATTTG	GTGATGGCATGGACTGTGGT

Table 7: Primers used for cloning.

S.No.	Primer	Forward primer	Reverse primer
1.	hECSIT	GAATTCATGAGCTGGGTCCAGGCCACC	AAGCTTGCTCTGGCCCTGCTGTC
2.	ECSIT/C14A	GCCTCGCAAGGGCCTGG	CCAGGCCCTTGCGAGGC
3.	ECSIT/C21A	GCACCGCAGGGGCCGCC	GGCGGCCCTGCGGTGC
4.	ECSIT/C43A	GGCCTCCACGCCAGCGCAGCT	AGCTGCGCTGGCGTGGAGGCC

6.2.21 List of Antibodies used in this work

Various antibodies were used in the western blotting technique to check the signaling pathway and their levels under the ECSIT knockdown condition. The list of antibodies had mentioned below in **Table 8.**

 Table 8: Antibodies used.

Antibody	Catalogue	Dilution
ECSIT	HPA042979/ ITT13748	1:2000
GAPDH	SC47724	1:2000
pJAK2 Y221	3774S	1:2000
pJAK2 Y1007/1008	3771S	1:2000
pSTAT3 Y705	9145	1:2000
pSTAT3 S727	9136S	1:2000
STAT3	9132	1:2000
pMEKK 3	SC28043	1:2000
pJNK	6254	1:2000
pERK 1/2	9101	1:2000
ERK ½	9102	1:2000
pYAP S127	4911	1:2000
YAP	14074	1:2000
Cyclin D1	SC246	1:2000
Cyclin E	SC25303	1:2000
Cyclin A	SC751	1:2000
Cyclin B1	SC7393	1:2000
PARP	9542	1:2000
Caspase 3	9665	1:2000
Bcl 2	SC492	1:2000
Beclin 1	3738S	1:2000
Atg 5	2630S	1:2000
Anti-Rabbit	1706515	1:20,000
Anti-Mouse	1706516	1:20,000

Results

7.1 In-silico modeling of ECSIT structure

The comparison of the proteins of interest with homologous proteins was used to model the three-dimensional structure. ECSIT exhibits less similarity with other proteins, and there are fewer homologs, hence homology threading was used as the technique. The alpha fold structure was taken and a refined three-dimensional structure was obtained by performing molecular dynamic simulations **Fig. 21A**. The models of the complete structure and N-terminal mitochondrial signal sequence were acquired and verified through the Ramachandran plot. The structure of ECSIT full-length wild type, cysteine to alanine mutant as well as N-terminal structures had shown in **Fig. 21B**.

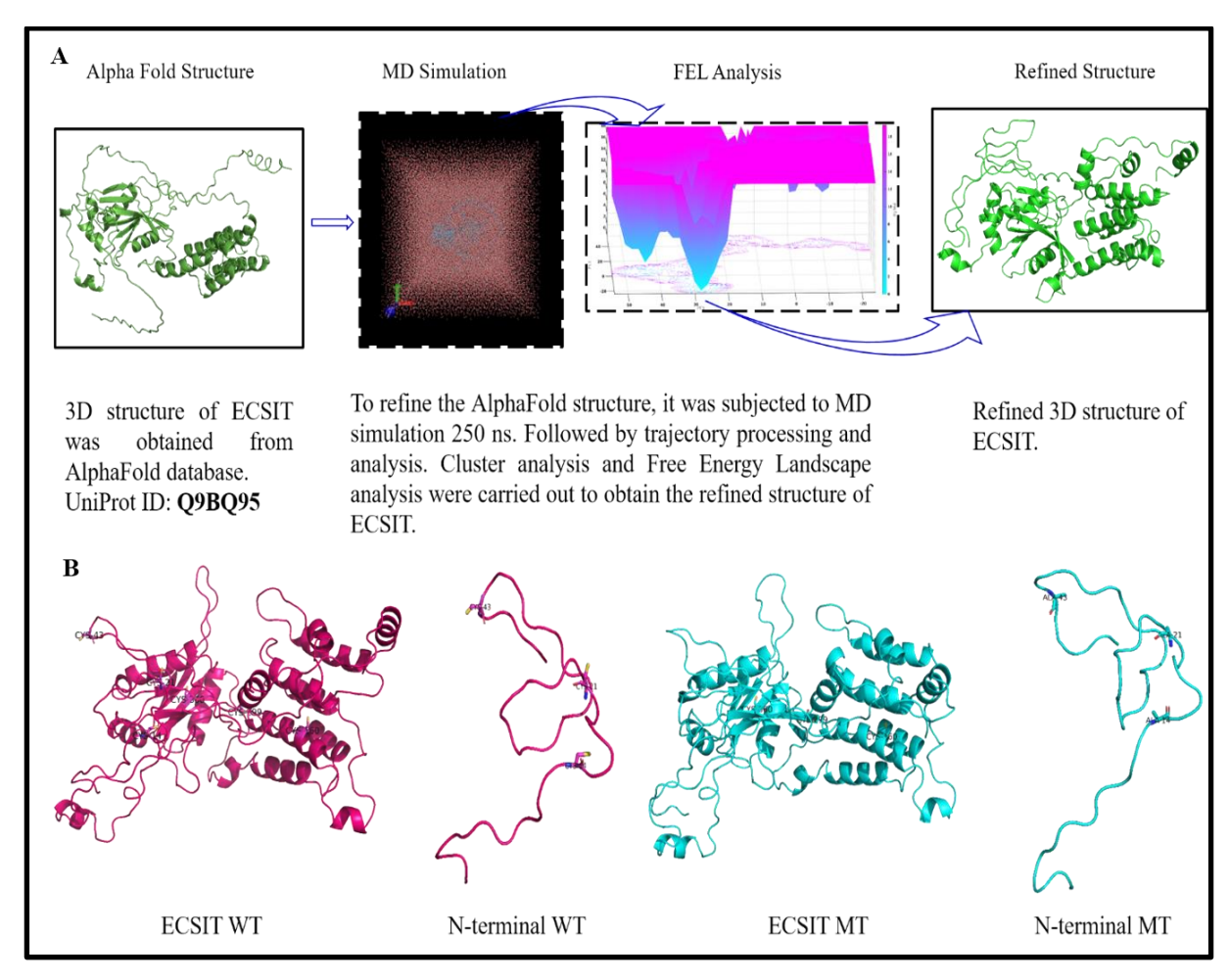
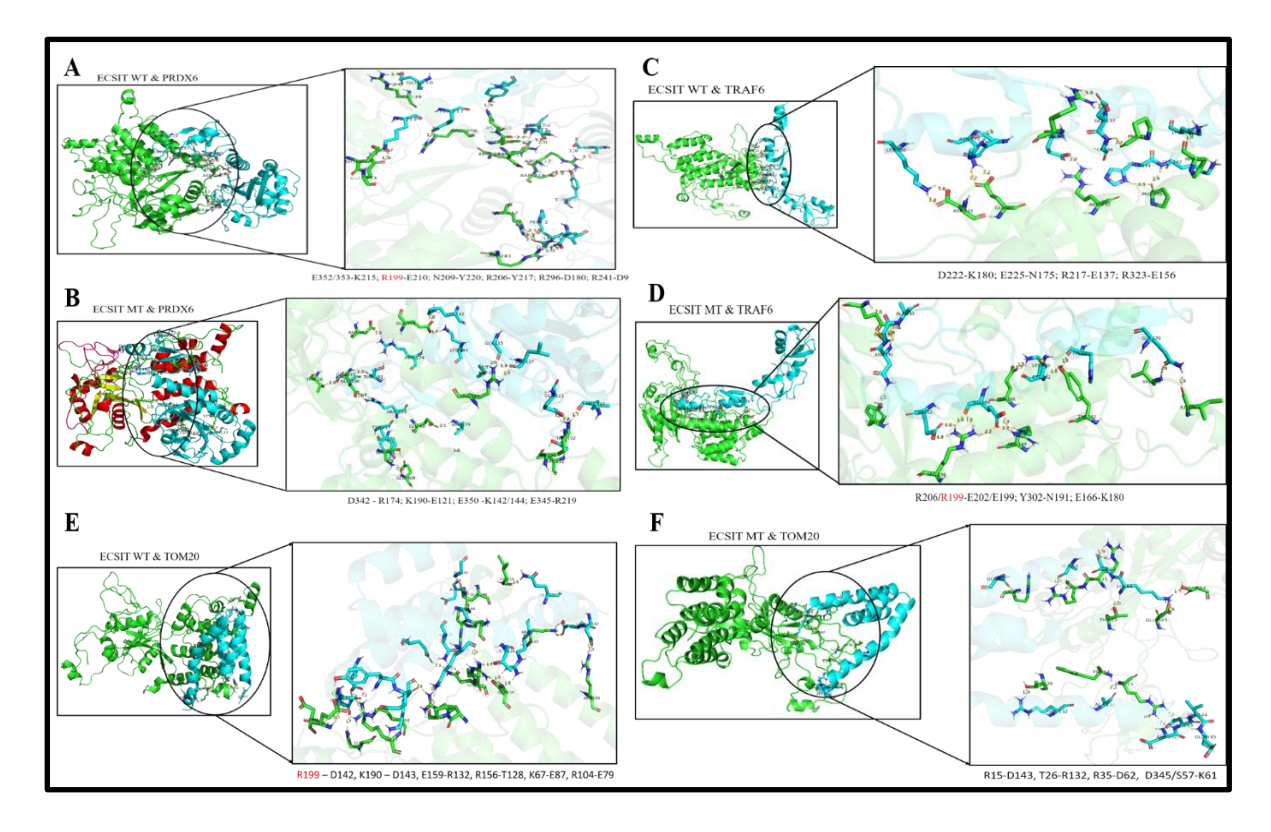


Fig. 21: Modeling of ECSIT N-terminal and three-dimensional whole protein structure. A) Workflow for *in-silico* analysis. B) Refined 3D structures of ECSIT Wild type, Mutant; N-terminal Wild type & Mutant.

7.2 Molecular dynamics simulation of ECSIT with other proteins shows preferential binding

The structural change affects the Co-localisation of protein. Indeed the conformational change depends on interacting partners. To check the conformation change of protein molecular dynamic simulation followed by protein-protein docking was performed. The side chain interactions of ECSIT WT with PRDX6 (E352/353-K215; R199-E210; N209-Y220; R206-Y217; R296-D180; R241-D9) **Fig. 22A**, ECSIT WT with TRAF6 (D222-K180; E225-N175; R217-E137; R323-E156) **Fig. 22C** and ECSIT WT with TOM20 (R199 – D142, K190 – D143, E159-R132, R156-T128, K67-E87, R104-E79) **Fig. 22E** shows preferential binding of ECSIT with PRDX6 and TOM20 with respect to R199 as it is shared amino acid residue. Whereas ECSIT MT with PRDX6 (D342-R174; K190-E121; E350 -K142/144; E345-R219) **Fig. 22B**, ECSIT MT with TRAF6 (R206/R199-E202/E199; Y302-N191; E166-K180) **Fig. 22D** and ECSIT MT with TOM20 (R15-D143, T26-R132, R35-D62, D345/S57-K61) **Fig. 22F** shows ECSIT MT had preferential binding with TRAF6 with respect to R199. The summary of sidechain interactions in the protein-protein docking study was shown in **Fig. 22G**.



 \mathbf{G}

ECSIT_Interaction Study		
Receptor	Ligand Name	Major Interaction Residues (Only side chain involving)
WT	PRDX6	E352/353-K215; R199-E210; N209-Y220; R206-Y217; R296-D180; R241-D9
	TRAF6	D222-K180; E225-N175; R217-E137; R323-E156
	TOM20	R199 – D142, K190 – D143, E159-R132, R156-T128, K67-E87, R104-E79
Mutant-Nterm	PRDX6	D342-R174; K190-E121; E350 -K142/144; E345-R219
	TRAF6	R206/R199-E202/E199; Y302-N191; E166-K180
	TOM20	R15-D143, T26-R132, R35-D62, D345/S57-K61

Fig. 22: Molecular dynamic simulations of ECSIT. (A, B) Protein Docking of ECSIT with Peroxiredoxin 6. (C, D) Protein Docking of ECSIT with TRAF6. (E, F) Protein Docking of ECSIT with TOM20. (G) Summary of Protein Docking studies of Wild type and mutant protein with its partner binding through side chain interactions.

7.3 *In-vitro* CD and Fluorescence spectroscopy data show a structural change with Hydrogen peroxide

As per the hypothesis, the alteration in protein structure under stress may be responsible for its localization to specific cell organelle and *in-silico* data suggests its structural change in

oxidized form compared to the wild-type protein. To validate this data in *in-vitro* we purified the native structure of protein along with mutants in E.coli using the Ni-NTA column. Various strategies were applied to obtain protein in supernatant fraction; different parameters such as a change in temperature, IPTG concentration, and change of host strain were used and shown in **Fig. 23A**. Out of all abundant amounts of protein in supernatant fraction obtained using arctic strain **Fig. 23B**. Protein purified from the supernatant fraction of arctic strain was functionally characterized using Circular dichroism (CD) and fluorescence spectroscopy techniques. The purified protein from the supernatant fraction of wild-type protein and N-terminal cysteine to alanine mutant of CD and fluorescence data suggests wild-type protein shows much secondary structural change in comparison with single, double, triple mutant under hydrogen peroxide treatment **Fig. 23C, D**.

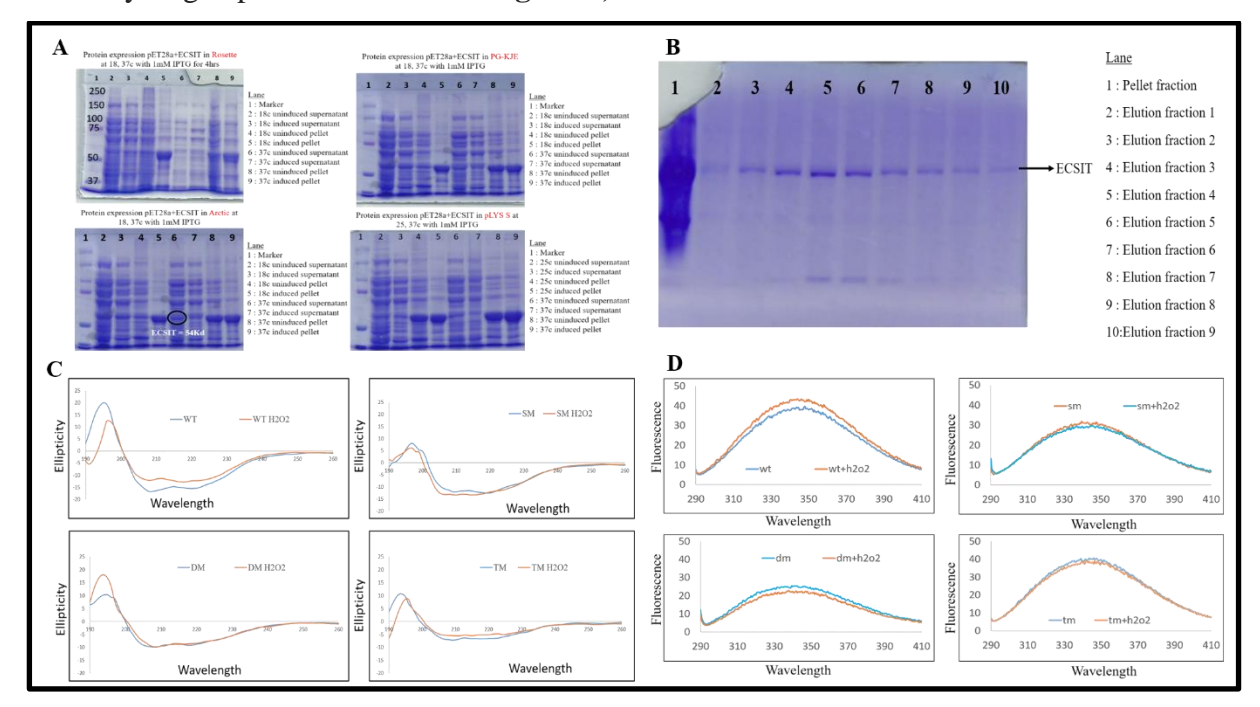


Fig. 23: The in-vitro purified protein shows structural alteration under hydrogen peroxide treatment. A) N-terminal cysteine mutants (Single (C14A) SM, Double (C14, 21A) DM, Triple (C14, 21,43A) TM) generated using overlap PCR method and workflow from generating mutant to purifying the protein. B) Protein expression in arctic strain and purification using Ni-NTA column. C) Circular Dichroism plots for wild-type, single, double and triple mutant protein with or without 1mM H₂O₂. D) Fluorescence spectroscopy data for purified wild type, single, double, and triple mutant with or without 1mM H₂O₂.

7.4 Import assay reveals wild-type protein translocates to mitochondria compared to triple mutant (C14,21,43A)

In-vitro CD and fluorescence data show secondary structural change under hydrogen peroxide treatment. To see whether the change in structure may alter its translocation to mitochondria, initially, ECSIT localization was checked by transfection with GFP plasmid and mitochondria with RFP plasmid and observed under fluorescence microscope **Fig. 24A** then we isolated mitochondria, the protein was incorporated with S³⁵ radioisotope, and import assay was performed to check its translocation **Fig. 24B.** Su9 DHFR was used as control and it shows wild type protein translocates better in comparison with mutant under 1mM H₂O₂ treatment.

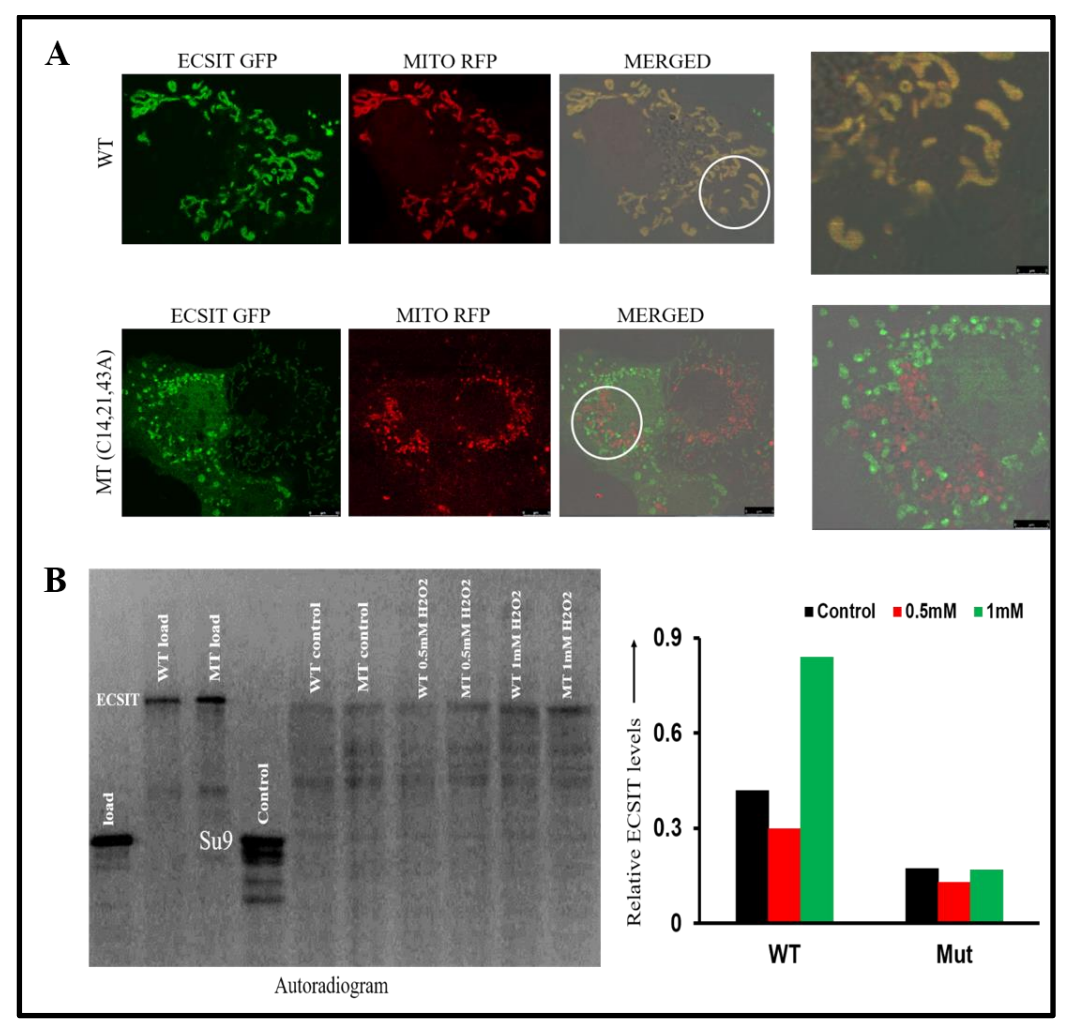


Fig. 24: Protein (ECSIT) is imported into Mitochondria. (A) Immunofluorescence detection of Wild type & Mutant protein Colocalisation to mitochondria. ECSIT cloned in GFPN1 vector and mitochondria stained in red color. (B) Autoradiogram of Import assay and densitometry graph.

Conclusions

- Lentivirus knockdown of ECSIT reveals a reduced proliferation rate of prostate cancer cells in DU145 & PC3.
- **2.** ECSIT modulates DU145 cell proliferation through JAK/STAT & HIPPO/YAP pathways whereas PC3 proliferates through HIPPO/YAP signaling pathway.
- **3.** Knockdown of ECSIT reveals delay in G1-S phase transition as evident from cyclin E expression.
- **4.** Knockdown of ECSIT induces autophagic cell death in DU145 whereas apoptotic cell death in PC3 cells.
- **5.** *In-silico* docking results represent preferential binding of ECSIT with partner binding proteins with respect to R199. For instance, wild-type protein preferentially with PRDX6 and TOM20 whereas mutant binds with TRAF6 and TOM20.
- **6.** *In-vitro* CD spectra reveal a change in ellipticity for wild type is more than mutant and fluorescence absorption spectra data reveals wild type protein had a variable structural change than mutant protein under oxidative stress.
- 7. Import assay data reveals wild-type protein localizes to mitochondria than mutant form.

Discussion

Cancer is a condition where cells lost their ability to control their replicative potential, resulting in increased cell proliferation and tumor formation. One of the causes of cancer is ROS which activates the internal signaling pathways of the cell such as the p38 MAPK pathway, Ras/Raf pathway, JAK/STAT pathway, etc...[100]. ROS makes a normal cell to adapted cancer cell and extreme ROS may lead to cell death by either apoptosis, autophagy, necroptosis, or ferroptosis [101]. Cancer cells have a death threshold level of ROS thereby showing a majority of the damaging signals [102]. Cancerous conditions were the result of reduced apoptosis, autophagy, and enhanced inflammatory signals, as well as oxidative stress, and the counteracting mechanisms, were done by exogenous sources through these potential mechanisms [103]. We were interested in studying the mechanism inside ECSIT and how they regulate the proliferation and growth of cancer cells because the role of ECSIT in the context of cancer had not been explored. The present study reveals the novel mechanisms of ECSIT in regulating cancer cell proliferation.

ECSIT had an augmented role in innate immunity by participating in TLR4 signaling whereby it complexes with TAK1 & TRAF6 and ubiquitination of ECSIT is necessary for NFkB activation which results in the upregulation of COX2 [7, 9, 33, 104] . TRIM59 has been known to inhibit this process [34]. ECSIT also known to be involved in interferon production via participating in RLR signaling [8]. ECSIT plays an essential role in developmental process through mesoderm formation [105], maintaining stem cell pluripotency [106] and regulating osteoblastic transdifferentiation [107]. ECSIT plays a role in the autophagy process where the proper assembly of mitochondrial complex I and proper Mitophagy occurs in its presence [17]. P62 [36], PRDX1 [25] and CRBN [37] are known to inhibit this process. ECSIT had a constructive role in mitochondria where cytosolic ECSIT localizes to mitochondria, helps in the mitochondrial fusion process, and aids in complex I formation by interacting with ACAD9 and NDUFAF1 proteins [6, 108, 109]. ECSIT ameliorates infections through the generation of mROS [23]; protects against corona virus [5], neurodegenerative disease [48], iron overload [50]; PRDX6 has been known to inhibit this process [10]. The physiological outcomes of this process by interacting with its partner binding proteins that were upregulated in various cancers by participating in various signaling pathways, which regulate cell proliferation we speculate its newly emerging role in cancer progression. The atlas database results provide us clues that ECSIT might participate in prostate cancer progression. This led to suspicion of the possibility

of ECSIT playing a mechanistic role in cancer, with cell proliferation, autophagy, and apoptosis being major focuses of interest. In search of mechanical aspects, a Lentiviral knockdown approach was used by selecting 3 targets on the ECSIT gene and validated using RT-PCR and western blotting. Knockdown of ECSIT depicts the reduced number of cells and this led to suspicion that the survival rate might be hampered. The cell survivability assay indicated us the survival rate was reduced in target 1 of DU145 cells and target 3 of PC3 cells. As cell proliferation depends on synchronized regulation of the cell cycle [110]. We suspect ECSIT might participates a role in cell cycle and to investigate this, synchronisation using nocodazole [111] was performed and the results illustrate us delay in cell cycle progression under knockdown conditions. To validate our results from FACS data, the levels of cell cycle marker proteins were compared for control and knockdown, confirming that t in comparisons with other cyclins, the cyclin E levels were varied in comparisons with other cyclins., we observed reduced JAK/STAT & HIPPO/YAP pathways under knockdown conditions in DU145 cells and these two pathways were critical for maintaining cell proliferation as upstream signaling pathways regulated the cyclins [112, 113]. Similarly, HIPPO/YAP pathway in PC3 cells. The participation of YAP protein in regulating tumorigenesis from the recent study strongly supports our results [114]. Our results demonstrate the knockdown of ECSIT delayed cell cycle progression from the G1-S phase. Besides hampered cell proliferation, cell death also contributes to the reduced number of cells under knockdown conditions and we suspect cell death might be due to autophagy or apoptosis. Previous research in macrophages and breast cancer cell lines has hinted that ECSIT contributes to autophagy or apoptosis. [17, 52]. To confirm the cell death pathways via ECSIT in prostate cancer models, we performed western blotting for marker proteins and results revealed that autophagic cell death occurs in DU145 and apoptotic cell death occurs in PC3 cells. The autophagic cell death mechanism was understood from previous studies by involving a key regulatory protein i.e. mTOR and results from our study indicated ERK/mTOR/ATG axis is critical for cell death. On the other hand, apoptotic cell death was mediated through PI3K/Akt pathway. The new evidence from recent publications suggests an association, which is consistent with our theory that ECSIT plays a vital function in cancer. [52, 53, 114, 115].

Although an antibacterial function of ECSIT was discovered many years ago [21], the relationship between ECSIT and oxidative stress remains unknown. Reports reveal that under oxidative stress conditions, NF-_kB translocates from the cytosol to the nucleus and AP endonuclease 1 and STAT3 translocate from the cytosol to mitochondria. The fate of ECSIT

under oxidative stress remains largely obscured. It is widely established from the literature that ECSIT interacts with TRAF6 for its translocation to the nucleus by ubiquitination [7]. As TRAF6 interaction leads to its translocation to the nucleus, there may be other binding partners that influence its translocation toward mitochondria. PRDX6 is another TRAF6 binding partner whose interaction competes with ECSIT. Thus, we speculate that ECSIT and PRDX6 interaction sequesters this complex to mitochondria for its function. Sequence analysis of ECSIT revealed 3 cysteines in the N-terminal mitochondrial signal sequence of ECSIT, which are thought to be sensitive to ROS-mediated modification. To unveil the role of ECSIT under oxidative stress conditions, first, the interrelation between ECSIT and ROS was examined by measuring the level of ROS upon ECSIT knockdown cells. The data revealed that the knockdown of ECSIT increases ROS levels. Upon establishing the concept that ECSIT regulates ROS levels, we then examined the partner-binding protein interactions through insilico analysis and validated it through in-vitro methods. WT ECSIT protein was modeled and built the structure for mutant ECSIT with all N-terminal cysteine residues to alanine. *In-silico* data revealed that ECSIT Wild type protein interacts with PRDX6 and TOM20 with respect to R199 residue during its translocation to mitochondria. Mutant ECSIT protein interacted with TRAF6 with respect to R199 and failed to translocate to mitochondria. Validation of *in-silico* was performed through in-vitro experiments using a bacterial vector expressing ECSIT with and without all cysteine residues by circular dichroism and fluorescence spectroscopy in the presence or absence of oxidizing agent (H₂O₂). Functional characterization of the purified protein shows that wild-type protein had a structural change upon treatment with an oxidizing agent compared with mutant protein in both circular dichroism and fluorescence spectroscopy. The structural change was further confirmed at the organelle level by performing an import assay [116, 117]. Oxidized WT-ECSIT protein translocated more to mitochondria compared with WT-ECSIT. However, mutants failed to translocate. Thus, these results suggest that oxidized ECSIT undergoes structural changes with enhanced interaction, thus leadings to translocation to the mitochondria.

Publications

- ➤ Chaitanya N.S.N., BM Reddy A. (2019) Pancreatitis: Clinical Aspects of Inflammatory Phenotypes. In: Nagaraju G., BM Reddy A. (eds) Exploring Pancreatic Metabolism and Malignancy. Springer, Singapore. ISBN 978-981-32-9392-2.
- ➤ Pandey M, Singh M, Wasnik K, Gupta S, Patra S, Gupta PS, Pareek D, Chaitanya NSN, Maity S, Reddy ABM, Tilak R, Paik P. Targeted and Enhanced Antimicrobial Inhibition of Mesoporous ZnO-Ag₂O/Ag, ZnO-CuO, and ZnO-SnO₂ Composite Nanoparticles. ACS Omega. 2021 Nov 16;6(47):31615-31631.
- ➤ Gorantla Sri Charitha, **Nyshadham S. N. Chaitanya**, Aramati Bindu Madhava Reddy (2022) LKB1/STK11 mediated Signal transduction in hepatocellular carcinoma In: Nagaraju G., Sarfraz Ahmad (eds) Theranostics and Precision Medicine for the Management of Hepatocellular Carcinoma. Academic Press. ISBN 978-0323992831.
- ➤ Chaitanya NSN, Tammineni P, Nagaraju GP, Reddy AB. Pleiotropic roles of evolutionarily conserved signaling intermediate in toll pathway (ECSIT) in pathophysiology. J Cell Physiol. 2022 Jul 19. doi: 10.1002/jcp.30832. Epub ahead of print. PMID: 35853181.

REFERENCES

- 1. Ge, Q., et al., Identification, characterization, and functional analysis of Toll and ECSIT in Exopalaemon carinicauda. Dev Comp Immunol, 2021. 116: p. 103926.
- 2. Qu, F., et al., Identification and function of an evolutionarily conserved signaling intermediate in Toll pathways (ECSIT) from Crassostrea hongkongensis. Dev Comp Immunol, 2015. 53(1): p. 244-52.
- 3. Song, W., et al., Characterization, molecular cloning, and expression analysis of Ecsit in the spinyhead croaker, Collichthys lucidus. Genet Mol Res, 2016. 15(1).
- 4. Terenina, E., et al., Differentially expressed genes and gene networks involved in pig ovarian follicular atresia. Physiol Genomics, 2017. 49(2): p. 67-80.
- 5. Yuan, J., et al., Co-Expression of Mitochondrial Genes and ACE2 in Cornea Involved in COVID-19. Invest Ophthalmol Vis Sci, 2020. 61(12): p. 13.
- 6. Vogel, R.O., et al., Cytosolic signaling protein Ecsit also localizes to mitochondria where it interacts with chaperone NDUFAF1 and functions in complex I assembly. Genes Dev, 2007. 21(5): p. 615-24.
- 7. Mi Wi, S., et al., Ubiquitination of ECSIT is crucial for the activation of p65/p50 NF-κBs in Toll-like receptor 4 signaling. Mol Biol Cell, 2015. 26(1): p. 151-60.
- 8. Lei, C.Q., et al., ECSIT bridges RIG-I-like receptors to VISA in signaling events of innate antiviral responses. J Innate Immun, 2015. 7(2): p. 153-64.
- 9. Wi, S.M., et al., TAK1-ECSIT-TRAF6 complex plays a key role in the TLR4 signal to activate NF-κB. J Biol Chem, 2014. 289(51): p. 35205-14.
- 10. Min, Y., et al., Peroxiredoxin-6 Negatively Regulates Bactericidal Activity and NF-κB Activity by Interrupting TRAF6-ECSIT Complex. Front Cell Infect Microbiol, 2017. 7: p. 94.
- 11. Sato, H., et al., Differential cellular localization of antioxidant enzymes in the trigeminal ganglion. Neuroscience, 2013. 248: p. 345-58.
- 12. Navarro-Yepes, J., et al., Antioxidant gene therapy against neuronal cell death. Pharmacol Ther, 2014. 142(2): p. 206-30.
- 13. Glasauer, A. and N.S. Chandel, Targeting antioxidants for cancer therapy. Biochem Pharmacol, 2014. 92(1): p. 90-101.

- 14. Heide, H., et al., Complexome profiling identifies TMEM126B as a component of the mitochondrial complex I assembly complex. Cell Metab, 2012. 16(4): p. 538-49.
- 15. Alston, C.L., et al., Biallelic Mutations in TMEM126B Cause Severe Complex I Deficiency with a Variable Clinical Phenotype. Am J Hum Genet, 2016. 99(1): p. 217-27.
- 16. McKenzie, M. and M.T. Ryan, Assembly factors of human mitochondrial complex I and their defects in disease. IUBMB Life, 2010. 62(7): p. 497-502.
- 17. Carneiro, F.R.G., et al., An Essential Role for ECSIT in Mitochondrial Complex I Assembly and Mitophagy in Macrophages. Cell Rep, 2018. 22(10): p. 2654-2666.
- 18. Karplus, P.A., A primer on peroxiredoxin biochemistry. Free Radic Biol Med, 2015. 80: p. 183-90.
- 19. Perkins, A., et al., Peroxiredoxins: guardians against oxidative stress and modulators of peroxide signaling. Trends Biochem Sci, 2015. 40(8): p. 435-45.
- 20. Rhee, S.G., et al., Controlled elimination of intracellular H(2)O(2): regulation of peroxiredoxin, catalase, and glutathione peroxidase via post-translational modification. Antioxid Redox Signal, 2005. 7(5-6): p. 619-26.
- 21. West, A.P., et al., TLR signalling augments macrophage bactericidal activity through mitochondrial ROS. Nature, 2011. 472(7344): p. 476-80.
- 22. Ding, D., et al., Role of evolutionarily conserved signaling intermediate in Toll pathways (ECSIT) in the antibacterial immunity of Marsupenaeus japonicus. Dev Comp Immunol, 2014. 46(2): p. 246-54.
- 23. Geng, J., et al., Kinases Mst1 and Mst2 positively regulate phagocytic induction of reactive oxygen species and bactericidal activity. Nat Immunol, 2015. 16(11): p. 1142-52.
- 24. Seo, J.H., C.S. Hwang, and J.Y. Yoo, MTFMT deficiency correlates with reduced mitochondrial integrity and enhanced host susceptibility to intracellular infection. Sci Rep, 2020. 10(1): p. 11183.
- 25. Min, Y., et al., Inhibition of TRAF6 ubiquitin-ligase activity by PRDX1 leads to inhibition of NFKB activation and autophagy activation. Autophagy, 2018. 14(8): p. 1347-1358.
- 26. Lin, Y., et al., Characterization of the immune defense related tissues, cells, and genes in amphioxus. Sci China Life Sci, 2011. 54(11): p. 999-1004.

- 27. Ding, D., et al., The ECSIT Mediated Toll3-Dorsal-ALFs Pathway Inhibits Bacterial Amplification in Kuruma Shrimp. Front Immunol, 2022. 13: p. 807326.
- 28. Gong, Y., et al., Exosomal miR-224 contributes to hemolymph microbiota homeostasis during bacterial infection in crustacean. PLoS Pathog, 2021. 17(8): p. e1009837.
- 29. Akira, S., S. Uematsu, and O. Takeuchi, Pathogen recognition and innate immunity. Cell, 2006. 124(4): p. 783-801.
- 30. Cai, X., Y.H. Chiu, and Z.J. Chen, The cGAS-cGAMP-STING pathway of cytosolic DNA sensing and signaling. Mol Cell, 2014. 54(2): p. 289-96.
- 31. Lin, S.C., Y.C. Lo, and H. Wu, Helical assembly in the MyD88-IRAK4-IRAK2 complex in TLR/IL-1R signalling. Nature, 2010. 465(7300): p. 885-90.
- 32. Kawasaki, T. and T. Kawai, Toll-like receptor signaling pathways. Front Immunol, 2014.5: p. 461.
- 33. Kopp, E., et al., ECSIT is an evolutionarily conserved intermediate in the Toll/IL-1 signal transduction pathway. Genes Dev, 1999. 13(16): p. 2059-71.
- 34. Kondo, T., M. Watanabe, and S. Hatakeyama, TRIM59 interacts with ECSIT and negatively regulates NF-κB and IRF-3/7-mediated signal pathways. Biochem Biophys Res Commun, 2012. 422(3): p. 501-7.
- 35. Kim, M.J., et al., p62 is Negatively Implicated in the TRAF6-BECN1 Signaling Axis for Autophagy Activation and Cancer Progression by Toll-Like Receptor 4 (TLR4). Cells, 2020. 9(5).
- 36. Kim, M.J., et al., p62 Negatively Regulates TLR4 Signaling via Functional Regulation of the TRAF6-ECSIT Complex. Immune Netw, 2019. 19(3): p. e16.
- 37. Kim, M.J., et al., CRBN Is a Negative Regulator of Bactericidal Activity and Autophagy Activation Through Inhibiting the Ubiquitination of ECSIT and BECN1. Front Immunol, 2019. 10: p. 2203.
- 38. Meng, H., et al., Synthetic VSMCs induce BBB disruption mediated by MYPT1 in ischemic stroke. iScience, 2021. 24(9): p. 103047.
- 39. Stewart, A., H. Guan, and K. Yang, BMP-3 promotes mesenchymal stem cell proliferation through the TGF-beta/activin signaling pathway. J Cell Physiol, 2010. 223(3): p. 658-66.

- 40. Zou, H. and L. Niswander, Requirement for BMP signaling in interdigital apoptosis and scale formation. Science, 1996. 272(5262): p. 738-41.
- 41. Kobayashi, T., et al., BMP signaling stimulates cellular differentiation at multiple steps during cartilage development. Proc Natl Acad Sci U S A, 2005. 102(50): p. 18023-7.
- 42. Heldin, C.H., K. Miyazono, and P. ten Dijke, TGF-beta signalling from cell membrane to nucleus through SMAD proteins. Nature, 1997. 390(6659): p. 465-71.
- 43. Moustakas, A. and C.H. Heldin, Ecsit-ement on the crossroads of Toll and BMP signal transduction. Genes Dev, 2003. 17(23): p. 2855-9.
- 44. Haass, C. and D.J. Selkoe, Soluble protein oligomers in neurodegeneration: lessons from the Alzheimer's amyloid beta-peptide. Nat Rev Mol Cell Biol, 2007. 8(2): p. 101-12.
- 45. Hardy, J. and D.J. Selkoe, The amyloid hypothesis of Alzheimer's disease: progress and problems on the road to therapeutics. Science, 2002. 297(5580): p. 353-6.
- 46. LaFerla, F.M., K.N. Green, and S. Oddo, Intracellular amyloid-beta in Alzheimer's disease. Nat Rev Neurosci, 2007. 8(7): p. 499-509.
- 47. Mattson, M.P., An ECSIT-centric view of Alzheimer's disease. Bioessays, 2012. 34(7): p. 526-7.
- 48. Soler-López, M., et al., Interactome mapping suggests new mechanistic details underlying Alzheimer's disease. Genome Res, 2011. 21(3): p. 364-76.
- 49. Chen, W.N., et al., Hepatitis B virus X protein increases the IL-1β-induced NF-κB activation via interaction with evolutionarily conserved signaling intermediate in Toll pathways (ECSIT). Virus Res, 2015. 195: p. 236-45.
- 50. Milward, E., et al., The nexus of iron and inflammation in hepcidin regulation: SMADs, STATs, and ECSIT. Hepatology, 2007. 45(1): p. 253-6.
- 51. Peyssonnaux, C., et al., TLR4-dependent hepcidin expression by myeloid cells in response to bacterial pathogens. Blood, 2006. 107(9): p. 3727-32.
- 52. Hu, Y., et al., ECSIT inhibits cell death to increase tumor progression and metastasis via p53 in human breast cancer. Transl Cancer Res, 2022. 11(4): p. 699-709.
- 53. Peiris, M.N., et al., Proteomic analysis reveals dual requirement for Grb2 and PLCγ1 interactions for BCR-FGFR1-Driven 8p11 cell proliferation. Oncotarget, 2022. 13: p. 659-676.

- 54. Bott, S.N.K.L., Prostate cancer. 2021.
- 55. Jain, S., S. Saxena, and A. Kumar, Epidemiology of prostate cancer in India. Meta Gene, 2014. 2: p. 596-605.
- 56. Taitt, H.E., Global Trends and Prostate Cancer: A Review of Incidence, Detection, and Mortality as Influenced by Race, Ethnicity, and Geographic Location. Am J Mens Health, 2018. 12(6): p. 1807-1823.
- 57. Giona, S., The Epidemiology of Prostate Cancer, in Prostate Cancer, S.R.J. Bott and K.L. Ng, Editors. 2021, Exon Publications

Copyright: The Authors.: Brisbane (AU).

- 58. Rawla, P., Epidemiology of Prostate Cancer. World J Oncol, 2019. 10(2): p. 63-89.
- 59. Timms, B.G., Prostate development: a historical perspective. Differentiation, 2008. 76(6): p. 565-577.
- 60. Borley, N. and M.R. Feneley, Prostate cancer: diagnosis and staging. Asian J Androl, 2009. 11(1): p. 74-80.
- 61. Saranyutanon, S., et al., Therapies Targeted to Androgen Receptor Signaling Axis in Prostate Cancer: Progress, Challenges, and Hope. Cancers (Basel), 2019. 12(1).
- 62. Giri, V.N., et al., Role of Genetic Testing for Inherited Prostate Cancer Risk: Philadelphia Prostate Cancer Consensus Conference 2017. J Clin Oncol, 2018. 36(4): p. 414-424.
- 63. Shah, A., et al., Mechanistic targets for BPH and prostate cancer—a review. Reviews on Environmental Health, 2021. 36(2): p. 261-270.
- 64. Hoang, D.T., et al., Androgen receptor-dependent and -independent mechanisms driving prostate cancer progression: Opportunities for therapeutic targeting from multiple angles. Oncotarget, 2017. 8(2): p. 3724-3745.
- 65. Saraon, P., et al., Mechanisms of Androgen-Independent Prostate Cancer. EJIFCC, 2014. 25(1): p. 42-54.
- Wang, G., et al., Genetics and biology of prostate cancer. Genes & development, 2018.32 17-18: p. 1105-1140.
- 67. Sobel, R.E. and M.D. Sadar, Cell lines used in prostate cancer research: a compendium of old and new lines--part 1. J Urol, 2005. 173(2): p. 342-59.

- 68. Prins, G.S. and O. Putz, Molecular signaling pathways that regulate prostate gland development. Differentiation, 2008. 76(6): p. 641-59.
- 69. Ramalingam, S., V.P. Ramamurthy, and V.C.O. Njar, Dissecting major signaling pathways in prostate cancer development and progression: Mechanisms and novel therapeutic targets. The Journal of Steroid Biochemistry and Molecular Biology, 2017. 166: p. 16-27.
- 70. Rybak, A.P., R.G. Bristow, and A. Kapoor, Prostate cancer stem cells: deciphering the origins and pathways involved in prostate tumorigenesis and aggression. Oncotarget, 2015. 6(4): p. 1900-19.
- 71. da Silva, H.B., et al., Dissecting Major Signaling Pathways throughout the Development of Prostate Cancer. Prostate Cancer, 2013. 2013: p. 920612.
- 72. Ramalingam, S., V.P. Ramamurthy, and V.C.O. Njar, Dissecting major signaling pathways in prostate cancer development and progression: Mechanisms and novel therapeutic targets. J Steroid Biochem Mol Biol, 2017. 166: p. 16-27.
- 73. Gallagher, R.P. and N. Fleshner, Prostate cancer: 3. Individual risk factors. Cmaj, 1998. 159(7): p. 807-13.
- 74. Griffiths, J.C. and L.M. Shaw, The Laboratory Diagnosis of Prostatic Adenocarcinoma. CRC Critical Reviews in Clinical Laboratory Sciences, 1983. 19(3): p. 187-204.
- 75. Campodonico, F., et al., Management of Prostate Cancer with Systemic Therapy: A Prostate Cancer Unit Perspective. Curr Cancer Drug Targets, 2021. 21(2): p. 107-116.
- 76. Brawerman, G., The isolation of RNA from mammalian cells. Methods Cell Biol, 1973. 7: p. 1-22.
- 77. Liu, X. and S. Harada, RNA isolation from mammalian samples. Curr Protoc Mol Biol, 2013. Chapter 4: p. Unit 4.16.
- 78. Liu, Z., et al., SLC4A4 promotes prostate cancer progression in vivo and in vitro via AKT-mediated signalling pathway. Cancer Cell Int, 2022. 22(1): p. 127.
- 79. Kumar, Y., A. Phaniendra, and L. Periyasamy, Bixin Triggers Apoptosis of Human Hep3B Hepatocellular Carcinoma Cells: An Insight to Molecular and IN SILICO Approach. Nutr Cancer, 2018. 70(6): p. 971-983.
- 80. Veronica, J., et al., Iron superoxide dismutase contributes to miltefosine resistance in Leishmania donovani. Febs j, 2019. 286(17): p. 3488-3503.

- 81. Jackman, J. and P.M. O'Connor, Methods for synchronizing cells at specific stages of the cell cycle. Curr Protoc Cell Biol, 2001. Chapter 8: p. Unit 8.3.
- 82. Ray, P.D., B.-W. Huang, and Y. Tsuji, Reactive oxygen species (ROS) homeostasis and redox regulation in cellular signaling. Cellular signalling, 2012. 24(5): p. 981-990.
- 83. Das, K. and A. Roychoudhury, Reactive oxygen species (ROS) and response of antioxidants as ROS-scavengers during environmental stress in plants. Frontiers in Environmental Science, 2014. 2.
- 84. Sies, H. and D.P. Jones, Reactive oxygen species (ROS) as pleiotropic physiological signalling agents. Nature Reviews Molecular Cell Biology, 2020. 21(7): p. 363-383.
- 85. Lam, C.R.I., et al., Loss of TAK1 increases cell traction force in a ROS-dependent manner to drive epithelial—mesenchymal transition of cancer cells. Cell Death & Disease, 2013. 4(10): p. e848-e848.
- 86. Park, S., et al., Long-term depletion of cereblon induces mitochondrial dysfunction in cancer cells. BMB Rep, 2021. 54(6): p. 305-310.
- 87. Bartolome, F., et al., Pathogenic p62/SQSTM1 mutations impair energy metabolism through limitation of mitochondrial substrates. Scientific Reports, 2017. 7(1): p. 1666.
- 88. Miwa, S., et al., Low abundance of the matrix arm of complex I in mitochondria predicts longevity in mice. Nat Commun, 2014. 5: p. 3837.
- 89. Canty, T.G., Jr., et al., Oxidative stress induces NF-kappaB nuclear translocation without degradation of IkappaBalpha. Circulation, 1999. 100(19 Suppl): p. Ii361-4.
- 90. Barchiesi, A., et al., Mitochondrial Oxidative Stress Induces Rapid Intermembrane Space/Matrix Translocation of Apurinic/Apyrimidinic Endonuclease 1 Protein through TIM23 Complex. J Mol Biol, 2020. 432(24): p. 166713.
- 91. Mohammed, F., et al., Rotenone-induced reactive oxygen species signal the recruitment of STAT3 to mitochondria. FEBS Lett, 2020. 594(9): p. 1403-1412.
- 92. Singh, S.P. and D.K. Gupta, A comparative study of structural and conformational properties of casein kinase-1 isoforms: insights from molecular dynamics and principal component analysis. J Theor Biol, 2015. 371: p. 59-68.
- 93. Bertero, A., S. Brown, and L. Vallier, Methods of Cloning. 2017. p. 19-39.

- 94. Chava, S., et al., A novel phosphorylation by AMP-activated kinase regulates RUNX2 from ubiquitination in osteogenesis over adipogenesis. Cell Death Dis, 2018. 9(7): p. 754.
- 95. Gopal, G.J. and A. Kumar, Strategies for the production of recombinant protein in Escherichia coli. Protein J, 2013. 32(6): p. 419-25.
- 96. Spriestersbach, A., et al., Chapter One Purification of His-Tagged Proteins, in Methods in Enzymology, J.R. Lorsch, Editor. 2015, Academic Press. p. 1-15.
- 97. Karri, S., et al., Adaptation of Mge1 to oxidative stress by local unfolding and altered Interaction with mitochondrial Hsp70 and Mxr2. Mitochondrion, 2019. 46: p. 140-148.
- 98. Dubey, S., M. Kallubai, and R. Subramanyam, Improving the inhibition of β-amyloid aggregation by withanolide and withanoside derivatives. Int J Biol Macromol, 2021.
 173: p. 56-65.
- 99. Roy, R.V., et al., Different roles of ROS and Nrf2 in Cr(VI)-induced inflammatory responses in normal and Cr(VI)-transformed cells. Toxicol Appl Pharmacol, 2016. 307: p. 81-90.
- 100. Perillo, B., et al., ROS in cancer therapy: the bright side of the moon. Experimental & Molecular Medicine, 2020. 52(2): p. 192-203.
- 101. Galadari, S., et al., Reactive oxygen species and cancer paradox: To promote or to suppress? Free Radical Biology and Medicine, 2017. 104: p. 144-164.
- 102. Vučetić, M., et al., The Central Role of Amino Acids in Cancer Redox Homeostasis: Vulnerability Points of the Cancer Redox Code. Front Oncol, 2017. 7: p. 319.
- 103. N, S.N.C., et al., Molecular mechanisms of action of Trehalose in cancer: A comprehensive review. Life Sci, 2021. 269: p. 118968.
- 104. Wadleigh, D.J., et al., Transcriptional activation of the cyclooxygenase-2 gene in endotoxin-treated RAW 264.7 macrophages. J Biol Chem, 2000. 275(9): p. 6259-66.
- 105. Xiao, C., et al., Ecsit is required for Bmp signaling and mesoderm formation during mouse embryogenesis. Genes Dev, 2003. 17(23): p. 2933-49.
- 106. Dinger, M.E., et al., Long noncoding RNAs in mouse embryonic stem cell pluripotency and differentiation. Genome Res, 2008. 18(9): p. 1433-45.

- 107. Bustos-Valenzuela, J.C., et al., Unveiling novel genes upregulated by both rhBMP2 and rhBMP7 during early osteoblastic transdifferentiation of C2C12 cells. BMC Res Notes, 2011. 4: p. 370.
- 108. Xu, L., et al., ECSIT is a critical limiting factor for cardiac function. JCI Insight, 2021. 6(12).
- 109. Xia, C., et al., Molecular mechanism of interactions between ACAD9 and binding partners in mitochondrial respiratory complex I assembly. iScience, 2021. 24(10): p. 103153.
- 110. Kaldis, P., Quo Vadis Cell Growth and Division? Frontiers in Cell and Developmental Biology, 2016. 4.
- 111. Ligasová, A. and K. Koberna, Strengths and Weaknesses of Cell Synchronization Protocols Based on Inhibition of DNA Synthesis. International Journal of Molecular Sciences, 2021. 22(19): p. 10759.
- 112. Canesin, G., et al., Cytokines and JAK/STAT signaling in prostate cancer: overview and therapeutic opportunities. Current Opinion in Endocrine and Metabolic Research, 2020. 10.
- 113. Jin, X., et al., YAP knockdown inhibits proliferation and induces apoptosis of human prostate cancer DU145 cells. Mol Med Rep, 2018. 17(3): p. 3783-3788.
- 114. Yang, S., et al., Key role for mitochondrial complex I assembly factor ECSIT and mitochondrial metabolism in controlling intestinal homeostasis and tumorigenesis by regulation of translation of YAP protein. 2022, Research Square.
- 115. Wen, H., et al., Recurrent ECSIT mutation encoding V140A triggers hyperinflammation and promotes hemophagocytic syndrome in extranodal NK/T cell lymphoma. Nat Med, 2018. 24(2): p. 154-164.
- 116. Murschall, L.M., et al., Protein Import Assay into Mitochondria Isolated from Human Cells. Bio Protoc, 2021. 11(12): p. e4057.
- 117. Schmidt, O., N. Pfanner, and C. Meisinger, Mitochondrial protein import: from proteomics to functional mechanisms. Nat Rev Mol Cell Biol, 2010. 11(9): p. 655-67.

Anti-Plagiarism Certificate

Molecular characteristics of ECSIT: Implications in Prostate cancer

by Nyshadham Sai Naga Chaitanya

Submission date: 06-Dec-2022 11:05AM (UTC+0530)

Submission ID: 1972939734

File name: Thesis-16LAPH04-Chaitanya.docx (17.69M)

Word count: 11838 Character count: 68323

Librarian

Indira Gandhi Memorial Library UNIVERSITY OF HYDERABAD Central University P.O. HYDERABAD-500 046.

Molecular characteristics of ECSIT: Implications in Prostate cancer ORIGINALITY REPORT STUDENT PAPERS **PUBLICATIONS** SIMILARITY INDEX INTERNET SOURCES PRIMARY SOURCES Nyshadham S. N. Chaitanya, Prasad Tammineni, Ganji Purnachandra Nagaraju, This similarity Aramati BM Reddy. "Pleiotropic roles of evolutionarily conserved signaling intermediate in toll pathway (ECSIT) in pathophysiology", Journal of Cellular I, leatity that Physiology, 2022 PhD Publication Submitted to University of Essex Student Paper Senthilmurugan Ramalingam, Vidya P. Ramamurthy, Vincent C.O. Njar. "Dissecting major signaling pathways in prostate cancer development and progression: Mechanisms and novel therapeutic targets", The Journal of Steroid Biochemistry and Molecular Biology, 2017 Publication

4

www.mdpi.com

Internet Source

5	Submitted to Manchester Metropolitan University Student Paper	<1%
6	hdl.handle.net Internet Source	<1%
7	krishikosh.egranth.ac.in	<1%
8	Submitted to University of Florida Student Paper	<1%
9	www.oalib.com Internet Source	<1%
10	Prostate Cancer Shifting from Morphology to Biology, 2013. Publication	<1%
11	journals.plos.org	<1%
12	Block, H "Production and comprehensive quality control of recombinant human Interleukin-1@b: A case study for a process development strategy", Protein Expression and Purification, 200802	<1%
13	Submitted to MAHSA University Student Paper	<1%
14	journal.waocp.org	

		<1%
15	scholarbank.nus.edu.sg	<1%
16	worldwidescience.org	<1%
17	www.science.gov Internet Source	<1%
18	www.xxhhjxhg.com Internet Source	<1%
19	id.scribd.com Internet Source	<1%
20	I Lakshmanan. "MUC16 induced rapid G2/M transition via interactions with JAK2 for increased proliferation and anti-apoptosis in breast cancer cells", Oncogene, 02/16/2012	<1%
21	Submitted to University of Sheffield Student Paper	<1%
22	www.jbc.org	<1%
23	Irina U. Agoulnik. "Coregulators and the Regulation of Androgen Receptor Action in Prostate Cancer", Androgen Action in Prostate Cancer, 2009	<1%

Exclude quotes

On

Exclude matches

< 14 words

Exclude bibliography On